This is to certify that the

dissertation entitled

NOISE AND VIBRATION DESIGN MODELING
WITH STATISTICAL ENERGY ANALYSIS

presented by

XIANLI HUANG

has been accepted towards fulfillment
of the requirements for

Ph.D. degree in MECHANICAL ENGINEERING

Clark Radcliffe
Major professor

Date June 24, 1994

NOISE AND VIBRATION DESIGN MODELING WITH STATISTICAL ENERGY ANALYSIS

By

Xianli Huang

A DISSERTATION

Submitted to
Michigan State University
in partial fulfillment of the requirements
for the degree of

DOCTOR OF PHILOSOPHY

Department of Mechanical Engineering

1994

ABSTRACT

NOISE AND VIBRATION DESIGN MODELING WITH STATISTICAL ENERGY ANALYSIS

By

Xianli Huang

Statistical Energy Analysis (SEA) was initially developed for predicting sound pressure and vibration levels in interior spaces and structures at audio frequencies. The work presented here includes important results on four topics: internal loss factor Identification, sound pressure sensitivity analysis, SEA response variance analysis and SEA response distributions. Internal loss factors for each element are identified from measured vibro-acoustic responses and the identified internal loss factors yield models which accurately predict vibro-acoustic responses. An SEA response sensitivity algorithm is formulated to relate variability of design parameters to SEA response variation. The method can be used to sort the design parameters which have greatest effects on sound pressure in acoustic spaces. The SEA response variance analysis relates response variances directly to variances of design parameters through linear approximation to SEA response variances. The SEA response distributions due to randomness of parameters are shown to be approximately Gaussian. The Gaussian distributions with the SEA response variance analysis provide a means to estimate the response confidence levels for existing SEA models or develop specifications on design parameters given variance specifications for sound and vibration performance. With these features SEA becomes a powerful tool for engineering acoustic design.

Copyright

Dedication

To my parents: H. Huang and W. Wang, to my wife: Xiaowei Li and to my daughters: SiRui and Rachel.

Acknowledgments

I would like to express my sincere appreciation to Professor Clark J. Radcliffe not only for his inspiration provoking advice all the way through the dissertation, for his training on me in professional faith, skills and insights of engineering, for his generous support, but also for his personal advice as a mentor. I would like to thank Dr. Joseph Wolf for his advice and help. I would like to thank Professor C. MacCluer for his advice and insight on derivations of SEA response distributions.

I would like to thank my committee members, Professors R. Rosenberg, A. Haddow and P.M. FitzSimons, for their advice, education, comments and help during my studies here.

I would like to thank my parents and sisters for their encouragement for my overseas studies. I would like to thank my father and mother-in-law, Mr. Zhou Li and Ms. L.M. Zheng, for taking care of my daughter in China when my wife and I were in The United States. I would like to thank my wife and my daughter for their support.

I would like to thank my officemate, Sachin Gogate for his friendship and his help over the years. I would like to thank my friends during my studies here. They include: Lu-ping Chao, Chris Eusebi, Blane Hansknecht, Steve Connolly, Jon Iwamasa, Chang-bo Chao, Jerome Palazzolo and Matt Brach.

Finally I gratefully acknowledge the technical assistance and support of Dr. Steve Rohde, Dr. P. Oh and Dr. Joseph Wolf of the General Motors Systems Engineering Center, especially for their discussions of statistical variances. I also gratefully acknowledge the assistance and support of Dr. W. Resh of Chrysler Technology Center.

LIST OF TABLES

LIST OF FIGURES

Chapter 1 Introduction

1.1 Statistical Energy Analysis (SEA) Overview

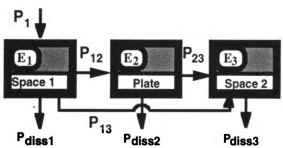

Figure 1.1 Conceptual SEA Model

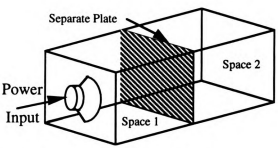

Figure 1.2 3-Element SEA Model Schematic

SEA can be illustrated with a simple SEA model: two spaces are separated by an aluminum plate (Figures 1.1 and 1.2). Stored energies are represented by E_1, E_2 and E_3 in the element blocks. Power flows between the elements are shown by the arrows labeled P_{12}, P_{13}, and P_{23} where the subscripts refer to the elements connected. The model includes one external power input, P_1. Power dissipated by damping and acoustic treatment is represented by P_{diss1}, P_{diss2} and P_{diss3}.

SEA model analysis is a set of simultaneous, frequency dependent, algebraic equations for total element energies.

$$\mathbf{N}(f_k,\mathbf{x})\mathbf{e}(f_k,\mathbf{x}) = \frac{1}{2\pi f_k}\mathbf{P}(f_k) \tag{1.1}$$

where $\mathbf{x} = [x_1 \ \cdots \ x_M]$, the vector of SEA design parameters

f_k is the k^{th} analysis band center frequency (Hz.)

$\mathbf{e}(f_k,\mathbf{x})$ is a modal energy vector (Joule Hz/mode),

$\mathbf{P}(f_k) = [P_1(f_k) \quad \cdots \quad P_K(f_k)]^T$, input power vector (Watt).

$\mathbf{N}(f_k,\mathbf{x})$ is a symmetric and diagonally dominant matrix.

η_i $= \eta_i(f_k,\mathbf{x})$, internal loss factors (non-dimensional)

η_{ij} $= \eta_{ij}(f_k,\mathbf{x})$, coupling loss factor (non-dimensional)

n_i $= n_i(f_k,\mathbf{x})$, the element modal density (mode/Hz) and

$\mathbf{N}(f_k,\mathbf{x})$ is a K xK symmetric, diagonally dominant and definite positive matrix.

$$\mathbf{N}(f_k,\mathbf{x}) = \begin{bmatrix} n_1\eta_1 + \sum_{j=2}^{K} n_1\eta_{1j} & \cdots & -n_1\eta_{1i} & \cdots & -n_1\eta_{1K} \\ \vdots & \ddots & \vdots & \iddots & \vdots \\ -n_1\eta_{1i} & \cdots & n_i\eta_i + \sum_{j=1}^{i-1} n_j\eta_{ji} + \sum_{j=i+1}^{K} n_i\eta_{ij} & \cdots & -n_i\eta_{iK} \\ \vdots & \iddots & \vdots & \ddots & \vdots \\ -n_1\eta_{1K} & \cdots & -n_i\eta_{iK} & \cdots & n_K\eta_K + \sum_{j=1}^{K-1} n_j\eta_{jK} \end{bmatrix} \tag{1.2}$$

The fundamental assumption of SEA is that the energies in all independent modes equalize at steady state within each, narrow, frequency band. Total energy in "i^{th}" element over "k^{th}" frequency band, $E_{i,k}(f_k,\mathbf{x})$, is derived from the product of the element's modal energy, $e_{i,k}(f_k,\mathbf{x})$, and modal density, $n_i(f_k,\mathbf{x})$.

$$E_{i,k}(f_k,\mathbf{x}) = n_i(f_k,\mathbf{x})e_{i,k}(f_k,\mathbf{x}) \tag{1.3}$$

The energy in the "i^{th}" element in the "k^{th}" frequency band is related to mean-squared pressure or velocity.

$$E_{i,k}(f_k,\mathbf{x}) = \begin{cases} \dfrac{V_i}{\rho_i c_i^2} p_{i,k}^2(f_k,\mathbf{x}) & \text{for acoustic space} \\ \\ m_i v_{i,k}^2(f_k,\mathbf{x}) & \text{for structure} \end{cases} \tag{1.4}$$

where V_i is acoustic volume (m^3), ρ_i is mass density $\left(kg/m^3\right)$

c_i is speed of sound in medium (m/s), m_i is mass (kg)

$p_{i,k}^2$ is expected value of ms sound pressure $\left(Pa^2\right)$.

$v_{i,k}^2$ is expected value of mean-squared velocity $\left(m^2/s^2\right)$.

Both mean-squared (total) acoustic pressure and mean-squared (total) velocity are the sums of independent frequency components in each frequency band.

$$\begin{cases} p_i^2(\mathbf{x}) = \sum_{k=1}^{N_f} p_{i,k}^2(f_k,\mathbf{x}) = \dfrac{\rho_i c_i^2}{V_i} \sum_{k=1}^{N_f} E_{i,k}(f_k,\mathbf{x}) \text{ for acoustic spaces} \\ v_i^2(\mathbf{x}) = \sum_{k=1}^{N_f} v_{i,k}^2(f_k,\mathbf{x}) = \dfrac{1}{m_i} \sum_{k=1}^{N_f} E_{i,k}(f_k,\mathbf{x}) \text{ for structures} \end{cases} \tag{1.5}$$

where: N_f is the number of response frequency bands.

1.2 New Developments for SEA

The new developments for SEA presented in this dissertation include optimal internal loss factor identification, total sound pressure sensitivity analysis, SEA response variance analysis, and confidence level prediction for SEA responses. These developments on SEA extend the SEA method into a powerful tool for engineering vibro-acoustic design and modeling at audio frequencies. The SEA developments allow users to obtain accurate SEA responses and sound pressure sensitivity to design parameter variations. Users can compute SEA response variances via design parameter variances and use the variances with the Gaussian distributions to compute SEA response confidence levels and/or develop design parameter specifications for SEA models.

Chapter 2 Identification of Internal Loss Factors of SEA*

2.1 Introduction

Statistical Energy Analysis (SEA) is becoming a powerful method for quality acoustic design of automobile vehicle acoustic spaces. SEA predicts vehicle sound pressure and vibration response levels and is most accurate at high frequencies where differential equation based methods often fail. The accuracy of SEA predictions are dependent on the accuracy of SEA model parameters, such as modal density, internal loss factor and coupling loss factor. SEA has a long usage history in aerospace and naval engineering and analytical expressions for SEA parameters are available for regular geometric shapes such as beams, plates, and volumes. Many of the structural details used by naval and aerospace engineers are not applicable to automobiles (Vail, C.F., 1972). Automobile structures are often made of spot welded sheet metals and the parameters for real assemblies are not accurately approximated by available idealized analytical model subsystems. Currently, measured data are not generally available for automotive vehicle structures. SEA models for automobile applications need to be validated with measured automotive vehicle responses and accurate automotive SEA model parameters determined.

2.2 SEA Parameters and Identification

Total energies are the mean-rms energies in each element. The input power is the external power into the element. The internal loss factors quantify the rates of energy dissipation from each element. The coupling loss factors govern the power flow from

* This Chapter is based on the paper titled "Identification of Internal Loss Factors During Statistical Energy Analysis of Automotive Vehicles" in Proceedings of the 1993 Noise and Vibration Conference, SAE P-264

one element to another. The SEA analysis problem is to use (1.1) and (1.3) to solve for the energy responses of each element given the element SEA parameters and input powers. The SEA parameter identification problem is an inverse problem which uses the power balance equations and measured values of element response energies and input powers to compute SEA parameter values. The SEA equations are linear in the SEA coefficients N_{ij}. For each test with a single measurable power input, a maximum of K values in the coefficient matrix **N** can be computed. With access to all element input powers , K independent tests are possible, and K^2 values in the coefficient matrix can be computed. For a general SEA model with all possible element connections, there are K internal loss factors, K modal densities and $[K(K-1)/2]$ independent coupling loss factors. For the simplest practical case of two elements $(K=2)$, there are five SEA parameters to identify at each band frequency: two internal loss factors, two modal densities and one coupling loss factor. With a two element model there are only four possible tests with which to find these parameters (Table 2.1). The noteworthy fact here is that independent identification of all SEA parameters requires models with three or more elements for a model when all element couplings are present.

Table 2.1 Number of Independent SEA Tests versus Model Size shows that for very small models it is impossible to identify all SEA parameters because there are more parameters than tests

Model Size K	Possible Tests K2	Loss Factors K	Modal Densities K	Coupling Factors $K(K-1)/2$	Total SEA Parameters $K(K+3)/2$	Equations-Parameters $K(K-3)/2$
1	1	1	1	0	2	-1
2	4	2	2	1	5	-1
3	9	3	3	3	9	0
4	16	4	4	6	14	2
5	25	5	5	10	20	5

Previous investigations of SEA parameter identification have assumed input power is measurable, SEA models limited to two or three elements and elements with regular geometric topology. Bies and Hamid (1980) conducted an situ experiment to identify

internal loss factors and the coupling loss factor for two coupled plates. Clarkson and Pope (1981) developed indirect experimental method to determine the modal density and internal loss factors for flat plates and cylinders. Ghering and Raj (1987) conducted an experimental investigation on a cylinder-plate-beam structure. Norton and Greenhalph (1986) identified the internal loss factors of lightly damped SEA model of a pipeline system by both steady-state power flow and burst random-noise techniques.

The work discussed here will discuss parameter verification for more general, and larger, SEA models. For this initial investigation only internal loss factors will be identified and the simplifying assumption will be made that all coupling loss coefficients are known . This assumption is justified for many structures because SEA coupling coefficients are related to structure geometry, mass and stiffness properties. These values are typically well determined by the structure's design. In contrast, structure energy dissipation models are typically not well determined by structure geometry and material properties. Structure energy dissipation models are more typically determined empirically and it is these dissipation models which are needed to determine the SEA internal loss factors. The discussion below will present a method for identifying the K independent SEA internal loss factors of a K element model from a test with one known power input through a single SEA element. Additionally, the measurement of input power is often difficult and the identification of input power from measured element energies will be presented.

2.3 Input Power and Optimal Internal Loss Factor Identification

SEA response energies, E_i, are measurable quantities in terms of rms vibration velocity and sound pressure level. In contrast input powers, P_i, are not easily measurable without using an impedance head and external excitation source. We will assume here that responses from all elements in an SEA model are measurable at each band center frequency of interest, and that all coupling loss factors and modal densities are known at these frequencies. For convenience, we will assume with generality that power is input to

element 1. We will now use the SEA model equations solve for input power to element one and internal loss factors for all other elements.

Rewrite the SEA equation (1.1) to explicitly remove the input element's energy response from the SEA coupling matrix.

$$\begin{Bmatrix} N_{11} \\ N_{12} \\ \vdots \\ N_{1K} \end{Bmatrix} e_1 + \begin{bmatrix} N_{12} & N_{13} & \cdots & N_{1K} \\ N_{22} & N_{23} & \cdots & N_{2K} \\ \vdots & \vdots & \ddots & \vdots \\ N_{K2} & N_{K3} & \cdots & N_{KK} \end{bmatrix} \begin{Bmatrix} e_2 \\ e_3 \\ \vdots \\ e_K \end{Bmatrix} = \begin{Bmatrix} \frac{P_1}{2\pi f} \\ 0 \\ \vdots \\ 0 \end{Bmatrix} \tag{2.1}$$

Removing the power input element's equation from the SEA model equations removes the input power from the model equations. The power input element's equation in (2.1) is rearranged to give the elements input power in terms of known element energies, coupling losses, and the input element's internal loss factor.

$$P_1 = 2\pi f \sum_{i=1}^{K} N_{1i} e_i \tag{2.2}$$

The internal loss factor for the powered element, η_1, appears in the right hand side of this equation in N_{11} and is needed to solve for input power, P_1. The internal loss factor for the powered element with unknown input power cannot be identified from measured element energies and we must use other methods to estimate it.

The remaining SEA model equations in rows 2 to K of (2.1) are rearranged in a symmetric form which parallels the original SEA model equation but has the SEA model size reduced by one.

$$\begin{bmatrix} N_{22} & N_{23} & \cdots & N_{2K} \\ N_{23} & N_{33} & \cdots & N_{3K} \\ \vdots & \vdots & \ddots & \vdots \\ N_{2K} & N_{3K} & \cdots & N_{KK} \end{bmatrix} \begin{Bmatrix} e_2 \\ e_3 \\ \vdots \\ e_K \end{Bmatrix} = -\begin{Bmatrix} N_{12} \\ N_{13} \\ \vdots \\ N_{1K} \end{Bmatrix} e_1 \tag{2.3}$$

The modified coupling matrix, $\tilde{\mathbf{N}}$ is produced by removing the row and column associated with the power input element. The reduced response energy vector, $\tilde{\mathbf{e}}$, is

produced by removing the power input element's energy. An equivalent power input vector, $\tilde{\mathbf{P}}$, is then written in terms of the input element's response energy, known coupling factors for that element and the input element's internal loss factor. The above formulation allows an SEA identification problem with unknown input power to be recast into the form (2.3) with known inputs.

$$\tilde{\mathbf{N}}\tilde{\mathbf{E}} = \tilde{\mathbf{P}} \tag{2.4}$$

where: $$\tilde{\mathbf{P}} = -\begin{Bmatrix} N_{12} \\ N_{13} \\ \vdots \\ N_{1K} \end{Bmatrix} e_1 = \begin{Bmatrix} -N_{12}e_1 \\ -N_{13}e_1 \\ \vdots \\ -N_{1K}e_1 \end{Bmatrix}$$

In the revised SEA model, the vector $\tilde{\mathbf{P}}$ is the new SEA model input vector.

Internal loss factors in SEA govern the power dissipation in SEA model element. The internal loss factors are defined by damping ratio for structures and reverberation time for acoustic volumes. No analytical expressions exist for damping ratios and reverberation times and they must be identified experimentally.

The optimal internal loss factor identification algorithm developed here identifies the internal loss factors in such a way that the internal loss factors yield SEA models which most accurately predict the total SEA energy responses. Optimal internal loss factor identification is achieved by three steps. Step 1 is to identify an initial internal loss factors in each frequency band from measured energies in each element, measured power inputs, analytical modal densities and coupling loss factors. Step 2 is to determine element-wise constant damping ratios for structures and reverberation times for acoustic spaces from the identified internal loss factors in step 1 by using the least square method. Step 3 uses the SEA model and optimizes constant damping ratios and reverberation times with step 2 initial values to minimize the mean squared (ms) normalized error between predicted and measured total energies. The internal loss factors obtained in the optimization process yield an SEA model which predict the SEA responses with the least difference from measured total energy responses. The algorithm is illustrated in Figure

2.1 and explained below in detail.

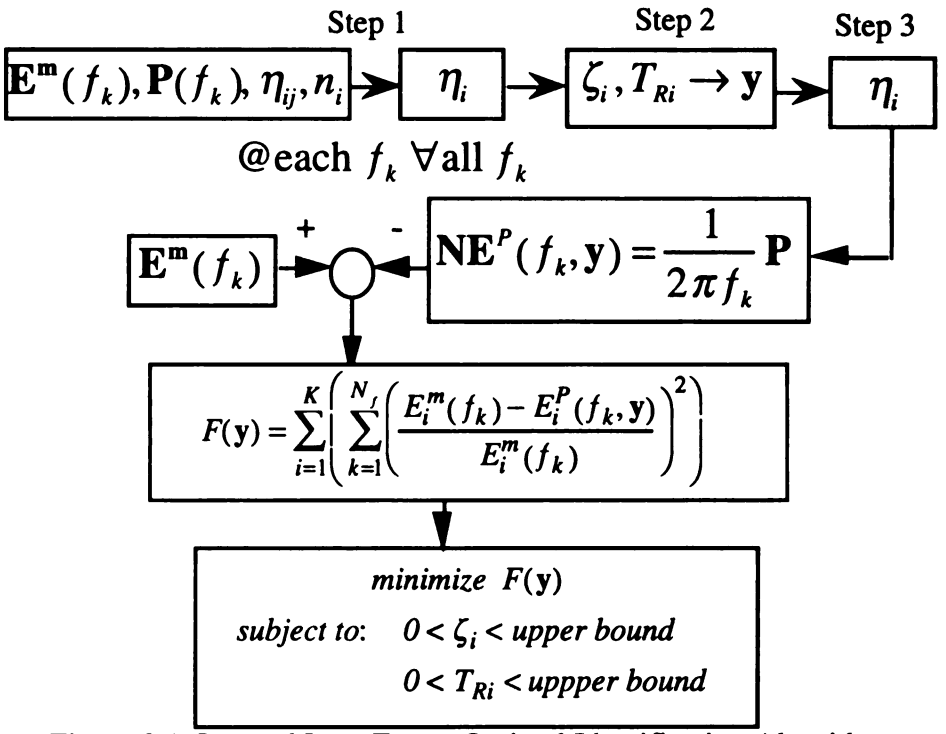

Figure 2.1 Internal Loss Factor Optimal Identification Algorithm

Step 1: Internal Loss Factor Identification. Internal loss factors in each frequency in each element can be solved as an inverse SEA problem from measured energy responses. Since the SEA equations are linear the internal loss factors can be determined uniquely from the measured energies, power inputs, analytical modal density and coupling loss factors.

To identify values for the internal loss factors, η_i, from measurements of the element energies, E_i, use (1.2) and solve for η_i in N_{ii} .

$$\eta_i = \frac{1}{n_i e_i}\begin{cases} \sum_{k=1}^{i-1} n_k \eta_{ki}(e_k - e_i) + \sum_{k>i}^{K} n_i \eta_{ik}(e_k - e_i) & i = 2, \cdots, K-1 \\ \sum_{k=1}^{K-1} n_k \eta_{ki}(e_k - e_i) & i = K \end{cases} \tag{2.5}$$

where: $e_i = E_i / n_i$

Step 2: Least Square Damping Ratios and Reverberation Time Computation. The damping ratios for structural element and reverberation time for acoustic spaces are assumed to be constant over all frequencies in an SEA model (Lyon, 1975). The element based damping, ζ_i, and reverberation time, T_{Ri}, can be determined from the identified frequency-dependent internal loss factors step 1 by minimizing the ms error.

Internal loss factors for acoustic spaces at frequency, f_k, are defined to be inversely proportional reverberation time, T_{Ri}, for the i^{th} element and at the k^{th} frequency, f_k.

$$\eta_i(f_k) = \frac{2.2}{T_{Ri} f_k} \tag{2.6}$$

where N_f is the number of frequencies

$\eta_i(f_k)$ is the identified internal loss factor for the i^{th} element at the k^{th} frequency

T_{Ri} is the reverberation time to be identified for he i^{th} element and

S is the mean squared difference

The reverberation time, T_{Ri}, can be found from the identified internal loss factors over N_f frequency bands by the least square method.

$$T_{Ri} = \frac{2.2 \sum_{j=1}^{N_f} 1/f_k^2}{\sum_{k=1}^{N_f} \eta_i(f_k)/f_k} \tag{2.7}$$

The internal loss factor for structure is defined to be twice of the damping ratio.

$$\eta_i(f_k) = 2\zeta_i \tag{2.8}$$

The ms difference between identified and computed internal loss factors can be written as:

$$S = \sum_{k=1}^{N_f} \left(\eta_i(f_k) - 2\zeta_i\right)^2 \tag{2.9}$$

The damping ratio can be found from the identified internal loss factors over N_f frequency bands by the least square method.

$$\zeta_i = \frac{1}{2N_f} \sum_{k=1}^{N_f} \eta_i(f_k) \tag{2.10}$$

Step 3: Optimization of Damping Ratio and Reverberation Time. This step optimizes the damping ratios and reverberation times to minimize the ms difference between predicted and measured total energy in the system. The constant damping ratios and reverberation time in step 2 are used as an initial estimation for the optimization. Let $\mathbf{y}$ be a vector whose components are damping ratios for structural elements and reverberation times for acoustic spaces in the SEA model. The predictions of SEA responses from the SEA model are functions of the vector $\mathbf{y}$. The objective function for the optimization is the normalized ms difference between predicted and measured total energy in the system.

$$F(\mathbf{y}) = \sum_{i=1}^{K} \left(\sum_{k=1}^{N_f} \left(\frac{E_i^m(f_k) - E_i^P(f_k, \mathbf{y})}{E_i^m(f_k)} \right)^2 \right) \tag{2.11}$$

where $E_i^m(f_k)$ is the measured energy in the i^{th} element at the k^{th} frequency f_k

$E_i^p(f_k, \mathbf{y})$ is the predicted energy in the i^{th} element at the k^{th} frequency f_k

The normalization is important for the objective function. The reason is that the energies in the elements near power input sources are larger than the energies in the elements which is far from the power input sources. The normalization will weigh the elements with smaller energy response equally in the optimization, otherwise, the difference will be dominated by the energies in a few elements near sources. The most

important elements often have the lowest element energies because they are the elements at the end of the power flow chain, e.g. a vehicle's interior.

2.4 Application Examples

The first example is a simple conceptual model (Figures 1.1 and 1.2) to illustrate the details of internal loss factor identification. The SEA model consists of two identical cubes, separated by an aluminum panel with a flanking path between the cubes to model energy transfer by paths other than through the panel. Acoustic powers are input to the space 1 and the working medium is air (Table A1 in Appendix A). Space #1 is designated as element 1, the panel as element 2 and space #2 as element 3. Geometric and Material properties are listed in Table A1 in Appendix. The pressures in Space #1 and #2 are 39.13 and 19.41 $\left(\mathrm{N}/m^2\right)$ respectively and the velocity in the plate is $8.85\times10^{-4}(m/s)$ at 5,000 Hz.

Computation of the SEA model parameters, such as modal densities and coupling loss factors for every element and coupling, is the first step in internal loss factor identification. The modal density (A1, Appendix A) for structural element 2 is

$$n_2 = \frac{\sqrt{3}A}{hc_l} = \frac{\sqrt{3}\bullet 0.5^2}{0.007\bullet 5182} = 11.9\times10^{-3} \ \text{(modes / Hz)} \tag{2.12}$$

The modal densities at 5,000 Hz.(A2, Appendix A) for acoustic elements 1 and 3 are

$$n_1 = n_3 = \frac{4\pi f^2 V}{c^3} + \frac{\pi f A_s}{2c^2} + \frac{L_e}{8c} = \frac{4\pi\bullet 5000^2\bullet 0.5^3}{344^3} + \frac{\pi\bullet 5000\bullet 1.5}{344^2} + \frac{6}{8\bullet 344} = 1.10 \ \text{(modes / Hz)} \tag{2.13}$$

The critical frequency is 1786 Hz. and the band frequency is 5,000 Hz.. The coupling loss factors (A3, Appendix A) from the structural element 2 to the acoustic element 3 are

$$\eta_{21} = \eta_{23} = \frac{\rho_{AIR} c_{AIR} A}{M_p \omega \left(1 - \frac{f_c}{f}\right)^{1/2}}$$

$$= \frac{1.244 \bullet 344 \bullet 0.25}{2700 \bullet 0.007 \bullet 0.25 \bullet 2\pi \bullet 5000 \bullet \sqrt{1 - \frac{1786}{5000}}} \tag{2.14}$$

$$= 9.0 \times 10^{-4}$$

The coupling loss factor from acoustic element 1 to the structural element 2 can be computed by the reciprocity relationship (Lyon, R.H., 1975).

$$\eta_{12} = \frac{n_2}{n_1} \eta_{21} = \frac{11.94 \times 10^{-3}}{1.1} 9.0 \times 10^{-4} \tag{2.15}$$

$$= 1.0 \times 10^{-5}$$

The coupling loss factor for the flanking path between element 1 and element 3 is assumed constant for this example.

$$\eta_{13} = 0.0001 \tag{2.16}$$

The internal loss factor identification is carried out by using (2.5) to compute the internal loss factors. For this example assume the measured energy values at 5,000 Hz.

$$E_1 = \frac{V}{\rho c^2} \langle p^2 \rangle = \frac{0.125}{1.244 \bullet 344^2} \langle 39.13^2 \rangle \tag{2.17a}$$

$$= 1.3 \times 10^{-3} \text{ (Joules / Hz.)}$$

$$E_2 = m \langle v^2 \rangle$$

$$= 2700 \bullet 0.0075 \bullet 0.5^2 \langle (8.85 \times 10^{-4})^2 \rangle \tag{2.17b}$$

$$= 3.7 \times 10^{-6} \text{ (Joules / Hz.)}$$

$$E_3 = \frac{V}{\rho c^2} \langle p^2 \rangle = \frac{0.125}{1.244 \bullet 344^2} \langle 19.41^2 \rangle \tag{2.17c}$$

$$= 3.2 \times 10^{-4} \text{ (Joules / Hz.)}$$

The element modal energies, e_i, are computed by dividing measured total energy, E_i, by the modal density, n_i.

$$e_1 = \frac{E_1}{n_1} = \frac{1.3\times10^{-3}}{1.1} \tag{2.18a}$$
$$= 1.2\times10^{-3} \text{ (Joules / mode)}$$

$$e_2 = \frac{E_2}{n_2} = \frac{4.0\times10^{-6}}{11.94\times10^{-3}} \tag{2.18b}$$
$$= 3.1\times10^{-4} \text{ (Joules / mode)}$$

$$e_3 = \frac{E_3}{n_3} = \frac{3.2\times10^{-4}}{1.1} \tag{2.18c}$$
$$= 3.0\times10^{-4} \text{ (Joules / mode)}$$

Equations (2.12) through (2.18) are substituted into (2.11) to yield the values of internal loss factors, η_2 and η_3.

$$\eta_2 = 8.1\times10^{-5}, \tag{2.19a}$$

$$\eta_3 = 3.1\times10^{-4}. \tag{2.19b}$$

The internal loss factor in element 1 cannot be independently computed because we have used measured energy in that element as our model input.

The second example is an automotive vehicle to further demonstrate the internal loss factor identification algorithm (Figures 2.2 and 2.3). The automotive vehicle SEA model consists of 11 elements. "ENGINE" represents the engine surface vibration, "ENGCOMP" represents the engine compartment acoustic pressure, "LRAIL" and "RRAIL" represent the frame vibration, "UNDCARVOL" represents the under car volume acoustic pressure, "HOOD" represents the hood vibration, "DASH" (dash panel) represents the front of dash vibration, "FLOORPAN" represents the floor panels vibration, "OVERCARVOL" represents the over car volume acoustic pressure, "BODYPAN" represents the body panels vibration and "INTERIOR" represents the car interior acoustic pressure. The engine is assumed to be the only noise source and every element has at least one path to another element in the model. The physical parameters are measured from the car and then used to compute modal densities and coupling loss factors. The vibro-

acoustic energies from every elements are measured and then used to identify the internal loss factors. The computed modal densities, coupling loss factors and identified internal loss factors are used to form the car SEA model. The power emitted by the engine surface is very difficult to measure, however the surface vibration can be easily measured through accelerometers on a dynamometer test.

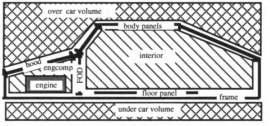

Figure 2.2 SEA Automotive Vehicle Model

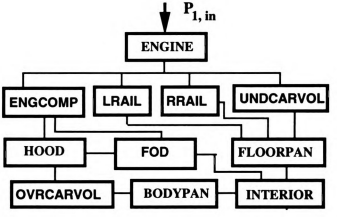

Figure 2.3 SEA Automotive Vehicle Model Element Coupling Chart

The laboratory test condition used was vehicle operation under load at 3000 rpm on a dynamometer. The RMS sound pressure levels in acoustic volumes and RMS acceleration levels in structural elements are measured in 4-12 spatial positions corresponding to each element in the model and the measured RMS velocity and pressure responses are used to identify the internal loss factors. The identified internal loss factors

for under car volume and front of dash are presented in Figures 2.4 and 2.5 respectively.

Constant internal loss factors for structural elements are typical modeling assumptions for most SEA models. Structural internal loss factor corresponds to twice the linear viscous damping ratio for these structures (Lyon, 1975). Identified internal loss factor values for our automotive structural element example show that the internal loss factors are not a constant at all frequencies. Specifically, the average internal loss factor for the front of dash (FOD) is 0.013 with a large standard deviation of 0.008 (Figure 2.5). The average internal loss factor for the FOD results corresponds to a damping ratio of 0.6% which is very small. There is no apparent trend in the identified internal loss factors for the FOD element and the other elements in our model displayed no regular trend as well This observation indicates that the actual internal loss factor values for automotive structural elements can not be accurately modeled either by Coulomb or viscous friction models. The very small damping measured may partially explain the inability to detect data trends. These results indicate that substantially more experience with identification

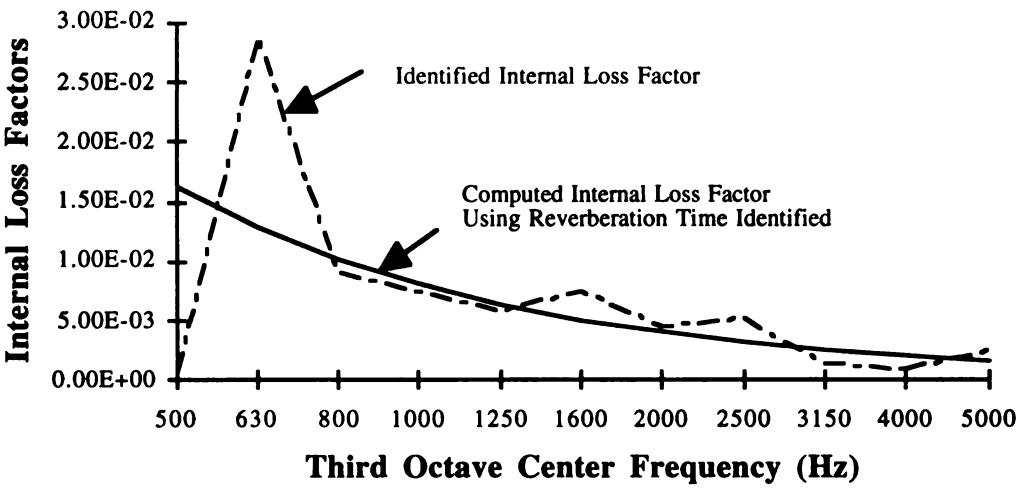

Figure 2.4 Identified and Computed Internal Loss Factors Using Computed Reverberation Time for Under Car Volume

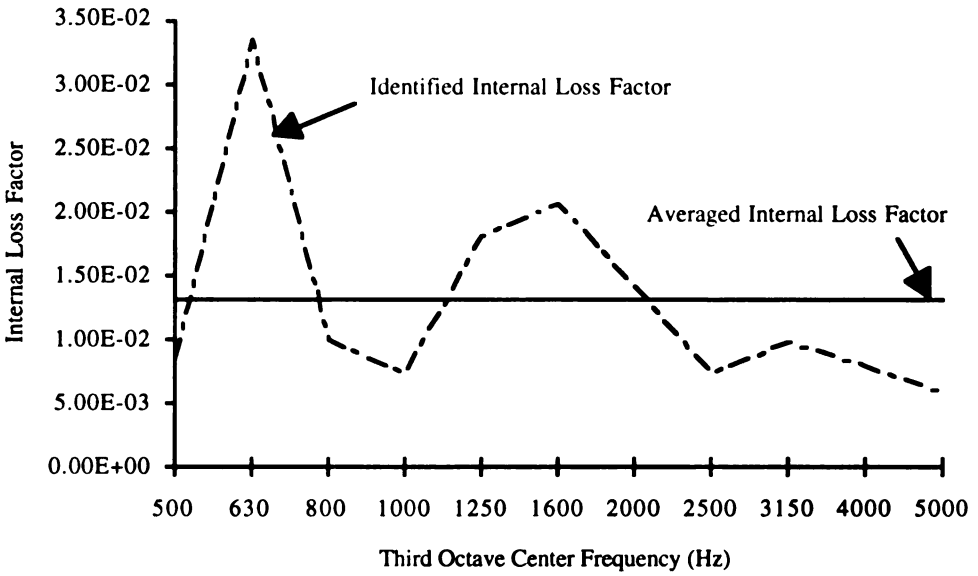

Figure 2.5 Identified and Average Internal Loss Factors for Front of Dash

of automotive structural dissipation is required before these sources of internal energy loss can be accurately modeled.

The internal loss factor for an acoustic element is often modeled using reverberation time (2.6). The identified internal loss factor values for the under car volume (UNDCARVOL) are presented in Figure 2.4. A least-squared-error fit to a reverberation time from the identified internal loss factors can be computed (2.7).

$$T_R = 0.27 \text{ (second)} \tag{2.20}$$

The internal loss factors computed (solid line) from the identified reverberation time are also presented in Figure 2.4 .

The acoustic internal loss factors identified for the under car volume (UNDCARVOL) for under car volume are very different from the reverberation time model at lower frequencies: 500 Hz. and 630 Hz. At higher frequencies: 800 to 5,000 Hz, identified internal loss factors closely match the trend corresponding to the values for a

reverberation time of 0.27 seconds. This result at high frequencies was true in general for other model acoustic volumes with the measured automotive data. These results indicate that a reverberation time based model of automotive vehicle acoustic spaces is appropriate at higher frequencies where modal density is larger. Our automotive data appeared to follow fixed reverberation times when modal densities were above approximately 0.5 modes per Hertz. Again, additional automotive data are required before modeling trends can be accurately determined.

Figure 2.6 Geo Metro Body Photo

An SEA model of a 1992 Geo Metro XFI body (Figure 2.6 and Figure 2.7) is used as the third example to illustrate the optimal internal loss factor identification algorithm. The Geo's engine, suspension and power train systems are removed and the body is supported by a frame support. The vehicle SEA model has 16 connectors and 8 elements. The structural elements, FOD, HOOD, FPAN and BPAN, represent dash panel, hood, floor panel and body panel surface vibration respectively. The acoustic spaces, ENGCMP, UND, OVER and INT, represent engine compartment, under car volume, over

car volume and interior acoustic pressure respectively. The physical design parameters and connectors for Geo SEA model are listed in Appendix B.

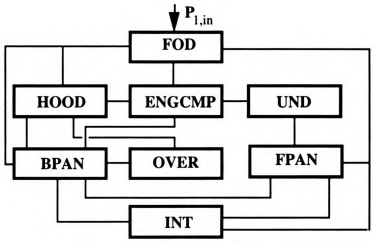

Figure 2.7 GEO METRO SEA Model Chart

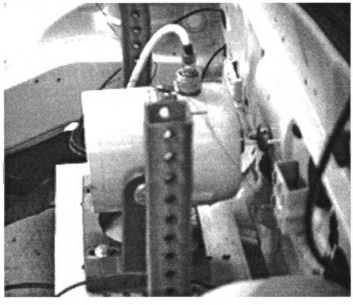

Figure 2.8 Vibrator Mount Assembly Photo

Tests of the Geo body were conducted in Controls Research Laboratory of the Department of Mechanical Engineering at Michigan State University. A Model 400 vibrator from Ling Dynamic Systems is mounted in the engine compartment (Figure 2.8).

The vibrator table is connected to the front of dash panel (FOD). The tests were conducted under two operating states: the two operating states were corresponding to two input signals. The operating state 1 is that the random signal was generated with an amplitude of 0.9 V over frequency range from 500 Hz. to 5000 Hz. from 35660A HP dynamic signal analyzer and sent to the vibrator through a power amplifier, Model PA100E from Ling Dynamic Systems. The operating state 2 is that the recorded Mazda 626 engine noise was played back to excite the GEO front of dash panel. The accelerations and SPL for all panels and acoustic spaces were measured for the operating state 1. The front of dash acceleration and interior SPL were measured for the operating state 2. The vibration signals were picked up by accelerometers between 6 and 16 locations for each structural elements. The sound pressures were picked up by microphones over 6-8 locations in each of the acoustic spaces. The measured accelerations and sound pressures were averaged over the measurement locations to obtain the mean values of the GEO vibro-acoustic responses corresponding to each model element. The standard deviations about the mean values were also computed from the measured responses over the different locations. The measured vibro-acoustic responses from the operating state 1 were used to generate the SEA model for the GEO through the optimal algorithm. The Mazda acceleration for front of dash panel was used as an input and was fed to the generated GEO SEA model to predict the interior SPL. The predicted interior was compared with the measured interior SPL. The measured SEA responses for all elements are shown in Appendix B. The optimal identification algorithm developed here was implemented in MATLAB.

Table 2.2 Identified and Optimized Damping Ratio and Reverberation Time

	FOD (%)	ENGCMP (second)	HOOD (%)	UND (second)	FPAN (%)	OVER (second)	BPAN (%)	INT (second)
identified	N/A	0.2907	33.65	0.3487	5.948	6.532	34.90	0.4111
optimized	N/A	0.4917	40.33	0.5914	3.997	6.3875	63.05	0.2111

The test data from the operating state 1 were used to identify the damping ratios and reverberation times in the optimization. The identified (from step 2) and optimized (in step 3) damping ratios and reverberation times are shown in Table 2.2. The damping ratios are not available for Front of Dash because the power input is unknown. the energy and damping ratio are model inputs.

Two GEO SEA models were formed by two sets of damping ratios and reverberation times obtained without (step 2) and with the optimization (step 3) respectively. The two GEO SEA models were used to predict the GEO vibro-acoustic responses. The predicted and measured ms responses were shown in Table 2.3. The results in Table 2.3 were plotted in Figure 2.9 for the SPL comparison and in Figure 2.10 for ms structural velocity comparison.

Table 2.3 Comparisons of Predicted and Measured Total Energies (in dB)

	Front of Dash	Engine Compartment	Hood	Under Car Volume	Floor Panel	Over Car Volume	Body Panel	Interior
measured	-66	88	-94	82	-90	80	-102	78
predicted (no optimal)	-66	84	-90	78	-91	79	-100	80
predicted (optimal)	-66	86	-91	81	-90	81	-102	78

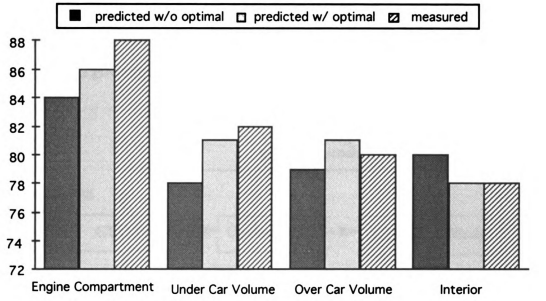

Figure 2.9 Geo Model Non-Optimal/Optimal/Measured SPL in dB of State 1

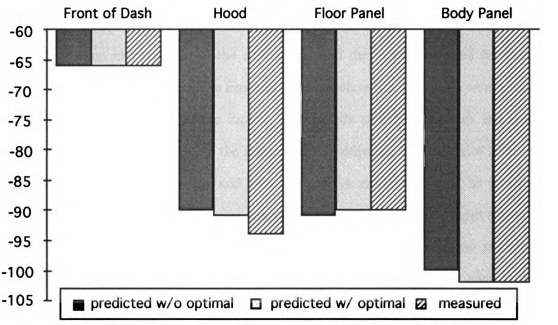

Figure 2.10 Geo Model Non-optimal/Optimal/Measured ms Velocity in dB(re 1 m/s)

The optimized damping ratio and reverberation time improved the accuracy of the

prediction. The improvement for the Hood and Floor Panel is 1 dB. There are 2 dB improvement in Engine Compartment, Body Panel and Interior and 3 dB improvement in Under Car Volume. The improvement on SEA prediction shows that the algorithm developed here is powerful.

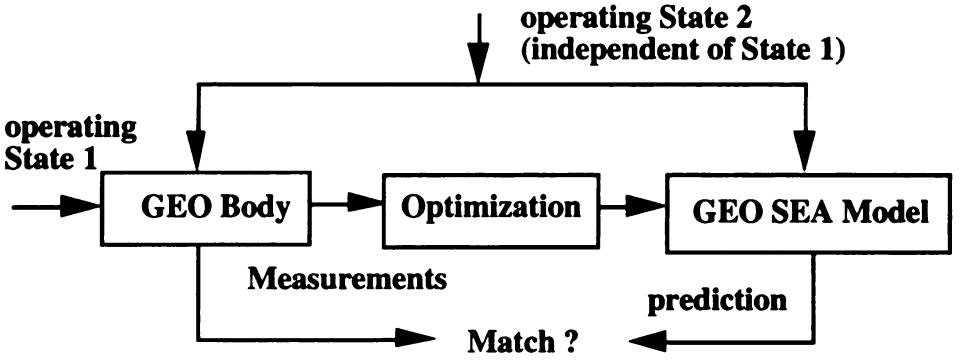

Figure 2.11 SEA Model Verification Procedure

The optimally generated SEA model for the GEO METRO body needs to be verified. The GEO METRO Front of Dash was excited by a Mazda 626 engine noise recording which is independent of the excitations and the responses used for the SEA internal loss factor optimization. The Front of Dash acceleration responses were measured and used as the SEA model power input. The Mazda power input was fed into the generated GEO SEA model to yield the interior SPL prediction. The interior SPL due to the Mazda excitation was measured and used as the SEA model output. The verification is to compare the GEO interior response prediction by the Mazda power input through the optimized SEA model to the measured GEO interior responses due to the same power input (see Figure 2.11). The predicted and measured interior SPL spectra were shown in Figure 2.12. The comparison shows that the predicted interior SPL is 74 dB and measured interior SPL is 75 dB. The predicted spectrum has good trend compared to the measured spectrum.

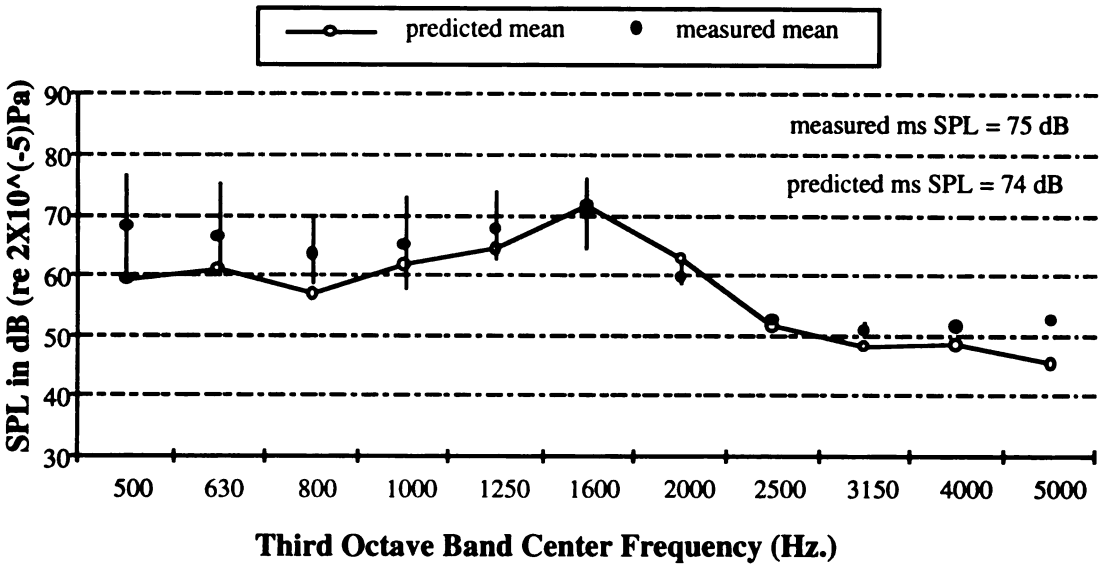

Figure 2.12 GEO SEA Model Verification Plot

2.5 Summary

The SEA internal loss factor identification problem for automotive vehicle model applications is addressed and an optimal algorithm for identifying the internal loss factors is developed. The optimal internal loss factor identification algorithm is demonstrated by both simple illustrative example and two more complicated automotive vehicle SEA models. Preliminary results for the identification without optimal process show that the common assumption of constant internal loss factors for structural elements may not accurately represent actual system responses, however, reverberation time models for acoustic volume elements are probably justified at higher frequencies. Additional automotive measurement experience is required before more accurate modeling trends can be determined. The results show and verify that the optimization on identification of damping ratios and reverberation time yields an SEA model which accurately predict the SEA model ms vibro-acoustic responses.

Chapter 3 Noise and Vibration Design Sensitivity from SEA*

3.1 Introduction

The SEA method predicts the expected value of vibro-acoustic response for modes grouped over a narrow frequency band. With the SEA assumption of equipartition of modal energy, this modal grouping significantly reduces the number of degrees of freedom in SEA models. The grouping also improves response prediction accuracy for modes with similar resonant frequencies through averaging of modal responses. The SEA method is a useful design tool for preliminary noise and vibration design studies because models can be developed at the prototype stage without detailed structural design specifications. Models can then be easily refined to increase prediction accuracy as the design matures. A specific example is the design of complex automotive structures.

SEA development started with prediction of the mean-rms values of vibro-acoustic response (Lyon, 1975). SEA response sensitivity analysis was initiated for optimal damping selection (Lu, 1987). This chapter will present a sound pressure (SP) sensitivity analysis method which relates SP variability to the variations in automotive vehicle model design parameters. The methodology proposed here can rank SP sensitivities and allow users to select the parameters which have the greatest effect on the SP in the vehicle interior.

SPL in an automotive vehicle interior is an accepted measure (ANSI S 1.4-1971) of perceived noise loudness and is used as one of the criteria for evaluating sound quality

---

* This Chapter is partially based on the paper titled " Sensitivity of the Statistical Energy Analysis for Automotive Vehicles, published in Proceedings of the Fourth Symposium on Advanced Technologies of the 1993 ASME Winter Annual Meeting

in many acoustic designs including automotive vehicle interiors. Acoustic design objectives often require that SPL be efficiently reduced as low as feasible. SPL is a logarithm of SP via a standard reference pressure, $P_{ref} = 20\mu P_a$. Reducing SP means reducing SPL. The question arises: "Which parameter in the vibro acoustic SEA model has the maximum effect on SP?"

3.2 Sound Pressure (SP) Sensitivity

SP sensitivity relates SP variations to the variability of design parameters. SP sensitivities quantify the effect of design parameters on acoustic performance. The design parameters which have greatest and least effect on SP can be determined by ranking the SP sensitivities to design parameters.

Sensitivity of a function F to its variable x is defined as (Frank, 1978):

$$S_x^F = \frac{\partial F/\partial x}{F/x} \tag{3.1}$$

SP Sensitivities, $S_{x_m}^{p^2(\mathbf{x})}$, with respect to a design parameter are derived by taking partial derivatives of (1.5) with respect to each design parameter and dividing by the ratio of the mean-squared pressure to that parameter.

$$\begin{aligned} S_{x_m}^{SP} = S_{x_m}^{p^2(\mathbf{x})} &= \frac{\partial p^2(\mathbf{x})/\partial x_m}{p^2(\mathbf{x})/x_m} = \frac{\sum_{j=1}^{N_f} \partial p^2(\mathbf{x}, f_j)/\partial x_m}{\sum_{j=1}^{N_f} p^2(\mathbf{x}, f_j)/x_m} \\ &= \frac{\sum_{j=1}^{N_f} \left(p^2(\mathbf{x}, f_j)/x_m\right)\left(\partial p^2(\mathbf{x}, f_j)/\partial x_m\right)/\left(p^2(\mathbf{x}, f_j)/x_m\right)}{\sum_{j=1}^{N_f} p^2(\mathbf{x}, f_j)/x_m} \\ &= \frac{\sum_{j=1}^{N_f} p^2(\mathbf{x}, f_j) S_{x_m}^{p^2(\mathbf{x}, f_j)}}{\sum_{j=1}^{N_f} p^2(\mathbf{x}, f_j)} \end{aligned} \tag{3.2}$$

The SP sensitivities, $S_{x_m}^{p^2(\mathbf{x})}$, has now been expressed in terms of the pressure sensitivities in each frequency band, $S_{x_m}^{p^2(\mathbf{x},f_j)}$. Sensitivity of the sound pressure $S_{x_m}^{p^2(\mathbf{x},f_j)}$ is equal to sensitivity of acoustic space energy, $E(\mathbf{x},f_j)$ in each frequency band.

$$S_{x_m}^{p^2(\mathbf{x},f_j)} = \frac{\partial p^2(\mathbf{x},f_j)/\partial x_m}{p^2(\mathbf{x},f_j)/x_m} = \frac{\partial E(\mathbf{x},f_j)/\partial x_m}{E(\mathbf{x},f_j)/x_m} = S_{x_m}^{E(\mathbf{x},f_j)} \tag{3.3}$$

SP sensitivity can now be expressed in terms of the sensitivities of energy in each frequency band by substituting (3.3) into (3.2).

$$S_{x_m}^{SP} = \frac{\sum_{j=1}^{N_f} E(\mathbf{x},f_j)\, S_{x_m}^{E_i(\mathbf{x},f_j)}}{\sum_{j=1}^{N_f} E(\mathbf{x},f_j)} = \sum_{j=1}^{N_f} \alpha_j S_{x_m}^{E(\mathbf{x},f_j)} \tag{3.4}$$

where $\alpha_j = \dfrac{E(\mathbf{x},f_j)}{\sum_{j=1}^{N_f} E(\mathbf{x},f_j)} < 1$ and $\sum_{j=1}^{N_f} \alpha_j = 1$

α_j is a normalized SP spectrum and represents a ratio of element energy in the j^{th} frequency band to the total energy over all frequency bands. SP sensitivity is therefore a weighted sum of sensitivities of total energies to the design parameters over all frequency bands. Frequency band energies are predicted by SEA equations and their sensitivities in each frequency band can be applied to the SP sensitivity analysis.

The sensitivity of the total energy is equal to the sum of the sensitivities of the modal energy and modal density because energy (1.3) is equal to product of modal energy and modal density (Frank, 1978).

$$\begin{aligned} S_{x_m}^{E(\mathbf{x},f_j)} &= \frac{\partial E(\mathbf{x},f_j)/\partial x_m}{E(\mathbf{x},f_j)/x_m} = \frac{\partial [n(\mathbf{x},f_j)e(\mathbf{x},f_j)]/\partial x_m}{n(\mathbf{x},f_j)e(\mathbf{x},f_j)/x_m} \\ &= S_{x_m}^{e(f_j,\mathbf{x})} + S_{x_m}^{n(f_j,\mathbf{x})} \end{aligned} \tag{3.5}$$

SP sensitivities can be expressed using (3.4-3.5) in terms of the sensitivities of the

modal energy and modal density.

$$S_{x_m}^{SP} = \sum_{j=1}^{N_f} \alpha_j \left[S_{x_m}^{e(\mathbf{x},f_j)} + S_{x_m}^{n(\mathbf{x},f_j)} \right] \tag{3.6}$$

SP sensitivity in an element depends on three terms in (3.6). The normalized SP spectrum, α_j, and modal energy response sensitivity, $S_{x_m}^{e(\mathbf{x},f_j)}$, are dependent upon system models and the modal density sensitivity, $S_{x_m}^{n(\mathbf{x},f_j)}$, is dependent upon element models only. Suppose that modal energy and modal density sensitivities in an element are computed for several design parameters and the sensitivity to a particular design parameter has the greatest value in all frequency bands, then one can say that design parameter has the greatest effect on SP without invoking (3.6) because α_j's are the same for those design parameters. This case is quite useful and convenient in early design stage.

Sensitivities of acoustic response modal energy, $e(\mathbf{x},f_j)$, and modal density, $n(\mathbf{x},f_j)$, to design parameters, $\mathbf{x}$, can be used to complete the analysis of SP sensitivities to design parameters. The sensitivity of modal density, $n(\mathbf{x},f_j)$, is defined by acoustic element definition equations. The sensitivity of acoustic modal energy, $e(\mathbf{x},f_j)$, requires derivatives obtained in the following section.

3.3 Modal Energy Derivatives to Parameter Variation

The SEA response derivatives are derived with the chain rule by using (1.3).

$$\frac{\partial E_i}{\partial x_m} = n_i \frac{\partial e_i}{\partial x_m} + \frac{\partial n_i}{\partial x_m} e_i \tag{3.7a}$$

$$\frac{\partial E_i}{\partial P_k} = n_i \frac{\partial e_i}{\partial P_k} + \frac{\partial n_i}{\partial P_k} e_i = n_i \frac{\partial e_i}{\partial P_k} \tag{3.7b}$$

The derivatives of modal energy to design parameters are found by taking derivatives on both sides of (1.1) with respect to the design parameters. Since the input power vector is independent of the design parameters, the partial derivative on the right hand side is zero. Two terms remain on the left hand side. Rearranging this result yields the derivatives of modal energy in matrix form.

$$\frac{\partial \mathbf{e}}{\partial x_m} = -\mathbf{N}^{-1}\frac{\partial \mathbf{N}}{\partial x_m}\mathbf{e} \tag{3.8}$$

Expanding partial derivative of matrix **N** with respect to each design parameters, x_m, in (3.8) through partial fraction expansion yields the results below.

$$\frac{\partial \mathbf{e}}{\partial x_m} = -\mathbf{N}^{-1}\left(\sum_{i=1}^{K}\sum_{j>i}^{K}\frac{\partial \mathbf{N}}{\partial \eta_{ij}}\mathbf{e}\frac{\partial \eta_{ij}}{\partial x_m} + \sum_{i=1}^{K}\frac{\partial \mathbf{N}}{\partial \eta_i}\mathbf{e}\frac{\partial \eta_i}{\partial x_m} + \sum_{i=1}^{K}\frac{\partial \mathbf{N}}{\partial n_i}\mathbf{e}\frac{\partial n_i}{\partial x_m}\right) \tag{3.9}$$

where $$\frac{\partial \mathbf{N}}{\partial \eta_{ij}} = \left[\frac{\partial N_{km}}{\partial \eta_{ij}}\right] = \begin{cases} n_i, & k = m = i \text{ or } k = m = j \\ -n_i, & k = i,\ m = j \text{ or } k = j,\ m = i \\ 0, & \text{otherwise} \end{cases}$$

$$\frac{\partial \mathbf{N}}{\partial \eta_i} = \left[\frac{\partial N_{km}}{\partial \eta_i}\right] = \begin{cases} n_i, & k = m = i \\ 0, & \text{otherwise} \end{cases}$$

$$\frac{\partial \mathbf{N}}{\partial n_i} = \begin{bmatrix} 0 & \cdots & & 0 & 0 & \cdots & 0 \\ \vdots & \ddots & & \vdots & \vdots & \iddots & \vdots \\ & & 0 & 0 & 0 & \cdots & 0 \\ 0 & \cdots & 0 & \left(\eta_i + \sum_{j=i+1}^{K}\eta_{ij}\right) & -\eta_{i,i+1} & \cdots & -\eta_{iK} \\ 0 & \cdots & 0 & -\eta_{i,i+1} & \eta_{i,i+1} & 0\cdots & 0 \\ \vdots & \iddots & \vdots & \vdots & 0 & \ddots & \vdots \\ & & & & \vdots & & 0 \\ 0 & \cdots & 0 & -\eta_{iK} & 0 & \cdots 0 & \eta_{iK} \end{bmatrix}$$

The beauty of the elegant forms of the SEA coefficient matrix **N** derivatives to SEA parameters is that they are easy to implement in computer algorithms.

The derivative of the modal energy vector, **e**, with respect to the element power inputs, P_i, is found by observing that the partial derivative of the power input vector, **P**, is non-zero in the i^{th} row only .

$$\frac{\partial \mathbf{e}}{\partial P_i} = \frac{1}{2\pi f_k}\mathbf{N}^{-1}\begin{Bmatrix} 0 \\ \vdots \\ 1 \\ \vdots \\ 0 \end{Bmatrix} \tag{3.10}$$

The partial derivatives of η_{ij}, η_i, and n_i are dependent on the specific element

definition equations.

3.4 Application of SP Sensitivity to Damping

Analysis of SP sensitivity to damping yields a quantitative evaluation of the effects of damping on SP in an SEA model acoustic space. Damping dissipates energy in each SEA model element. Damping is typically quantified in SEA models through each element's internal loss factor, η_i. Increasing the damping will increase the energy dissipation, decrease the SEA energy response and reduce the SP in the interior. Without loss of generality, it is assumed that

1. the SEA model has K elements,
2. a single input source drives the first element of the SEA model,
3. the SEA model is irreducible (at least one path from each element to any other element in the model),
4. the K^{th} element is an acoustic space, and
5. the design parameters, x_m, are internal loss factors, η_m.

The design goal is to find the internal loss factors which have the greatest effect on the SPL in the last acoustic element. The goal requires the evaluation of sensitivity of SPL to internal loss factors. Since the modal density is independent of internal loss factors, $S_{\eta_m}^{n_i} = 0$, the sensitivity of SP (3.6) can be written as:

$$S_{\eta_m}^{SP} = \sum_{j=1}^{N_f} \alpha_j S_{\eta_m}^{e_K} \tag{3.11}$$

The derivative of the interior modal energy, $e_K(\mathbf{x}, f_j)$, to the m^{th} internal loss factor, $\eta_m(\mathbf{x}, f_j)$, can be found by taking $i=m$ and selecting the last entry in the vector $S_{\eta_m}^{\mathbf{e}}$ in (3.9).

$$\frac{\partial e_K(\mathbf{x}, f_j)}{\partial \eta_m(\mathbf{x}, f_j)} = -\mathbf{N}_{Km}^{-1} n_m(\mathbf{x}, f_j) e_m(\mathbf{x}, f_j) \tag{3.12}$$

where $\mathbf{N}_{Km}^{-1}$ is the K^{th} row and m^{th} column entry in the $\mathbf{N}^{-1}$.

Note that one of the above derivatives exists for each of the internal loss factors in the SEA model.

The modal energy response can be expressed under the above five assumptions for (1.1) as

$$e_m(\mathbf{x}, f_j) = \frac{p_1(f_j)}{2\pi f_j}\mathbf{N}_{m1}^{-1} \quad \text{for m} = 1,2,\cdots,\text{K} \tag{3.13}$$

The sensitivities of the K^{th} modal energy response, $e_K(\mathbf{x}, f_j)$, to any internal loss factor, $\eta_m(\mathbf{x}, f_j)$, can be written as:

$$S_{\eta_m}^{e_K} = -\mathbf{N}_{Km}^{-1}(\mathbf{x}, f_j)n_m(\mathbf{x}, f_j)\mathbf{N}_{m1}^{-1}(\mathbf{x}, f_j)\Big/\left(\mathbf{N}_{K1}^{-1}(\mathbf{x}, f_j)\Big/\eta_m(\mathbf{x}, f_j)\right) \tag{3.14}$$

The rankings of the SP sensitivities in the interior to internal loss factors are useful for evaluating acoustic design strategies. SP sensitivities can be obtained by substituting (3.14) into (3.6) noting that the sensitivity of modal density to any internal loss factor is zero because modal density definitions are all independent of internal loss factor. The ranking of the SP sensitivities is determined by sorting the sensitivities of the modal energy to different internal loss factors. This sorting is typically frequency dependent. The sensitivities of the modal energy responses for a one-input SEA model are only associated with the entries in $\mathbf{N}^{-1}$ and invariant with the input power level.

The sensitivities of any modal energy responses to the source element internal loss factor, η_1, is derived by letting $m = 1$ in (3.14).

$$S_{\eta_1}^{e_i} = -\eta_1(\mathbf{x}, f_j)n_1(\mathbf{x}, f_j)\mathbf{N}_{11}^{-1}(\mathbf{x}, f_j) \tag{3.15}$$

The importance of (3.15) is that the sensitivities of all elements in our assumed SEA model topology to the source internal loss factor, $\eta_1(\mathbf{x}, f_j)$, are equal. The change of the source element internal loss factor will proportionally change the energy levels in all elements. Since the all energy levels are associated linearly by the SEA equations and the all other elements get their energy through the paths connected to the powered element, the sensitivities of all elements to the internal loss factor are the same.

3.5 Additional Design Examples

Two examples are used here to demonstrate the sensitivity analysis. The first example is a simple 3-element SEA model (Figures 1.1 and 1.2). We will illustrate the SPL sensitivity analysis in space 2 to damping parameters in detail. All parameters are listed in Appendix A. The second example is derived from a model of a production vehicle and more complex in structure (Figure 2.2 and 2.3). The model includes 11 elements, 15 couplings and 140 parameters. Although there are too many parameters to be listed here, the second example demonstrates the utility of SP sensitivity analysis for vehicle interior acoustic design.

The goal for the first example is to evaluate which element damping has the greatest effect on SP in element 3. Since modal density is independent of damping parameters, the term $S_{\mathbf{x}}^{n_3} = 0$ and (3.6) becomes:

$$S_x^{SP} = \sum_{j=1}^{N_f} \alpha_j S_x^{e_3} \tag{3.16}$$

The modal energy sensitivity frequency components in Space 2 with respect to internal loss factors are evaluated in (3.14) by taking K=3 and m=1, 2 ,3. Internal loss factors are characterized differently in acoustic and structural elements (Lyon, 1975). Internal loss factor for an acoustic space is inversely proportional to acoustic reverberation time. Internal loss factor for a structural element is directly proportional to damping ratio. The derivatives of internal loss factors with respect to reverberation times in acoustic spaces and plate are computed from (A4, Appendix A).

The absolute values of modal energy sensitivity frequency components in space 2 to reverberation times in acoustic elements 1 and 3 and damping ratio in the structural element 2 are plotted in Figure 3.1.

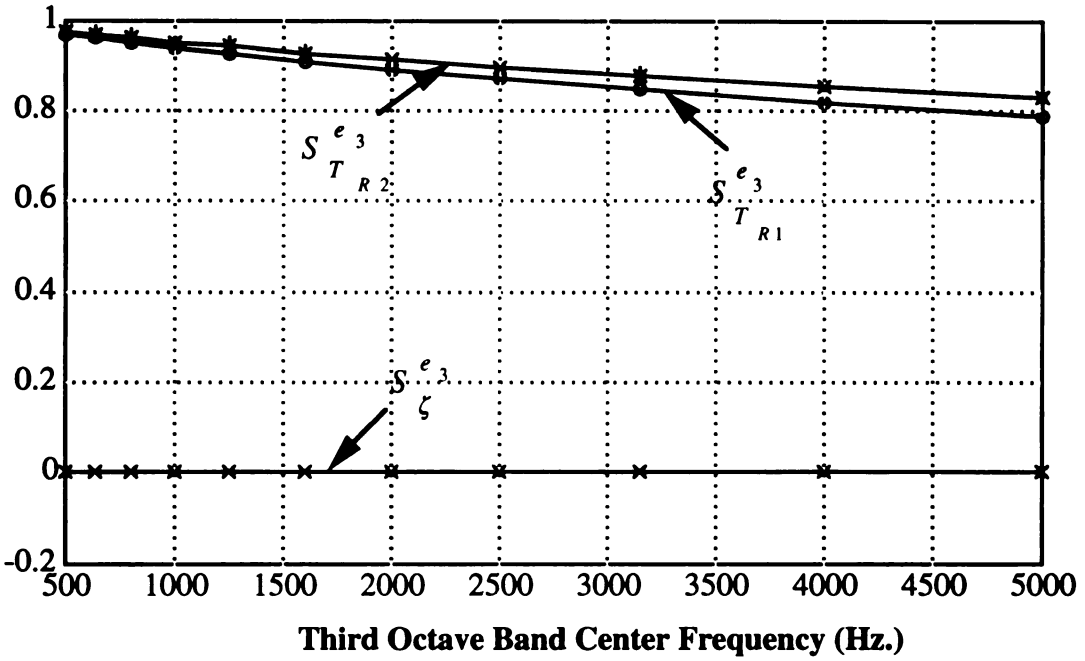

Figure 3.1 Modal Energy Sensitivities in Space 2 to Damping Parameters

Result examination in Figure 3.1 shows that the reverberation time in both acoustic spaces have the largest sensitivities over all frequency bands. The reverberation time in space 2 is less than the reverberation time in space 1 and has a larger effect on the responses in the space 2. The acoustic space 2 responses have the least sensitivity to the plate damping because the flanking path carries more power into space 2 than the plate. Since the reverberation times in space 2 and 1 have the greatest and second greatest and plate damping has the least sensitivities respectively over all frequency bands, from the modal energy frequency component sensitivities one can get some conclusion of effects of the design parameters on SP without computing SP sensitivity in (3.16). The conclusion is that decreasing reverberation time through acoustic treatment is the most efficient way to reduce the SP in space 2 and that increasing damping in the plate has the least effect on the SP in space 2.

The second example is an automotive vehicle (Figures 2.2 and 2.3). Note that,

although right and left frame rail are symmetric in the model and have identical geometric parameters, the measured responses are not the same for the two rails. Therefore the internal loss factors are not identified the same and this will lead to different SP sensitivities. The SP sensitivities of the interior acoustic responses to the internal loss factors are computed based on the SEA model.

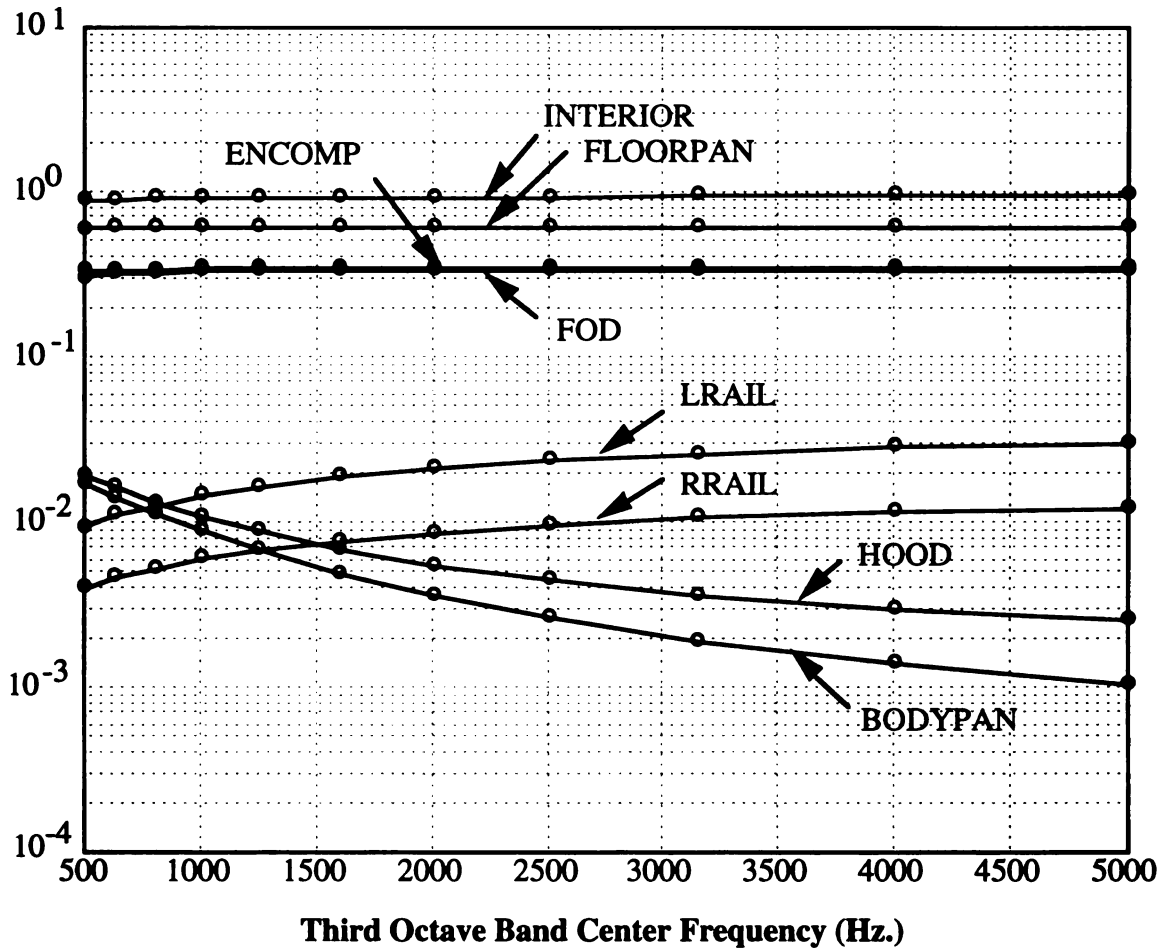

Figure 3.2 Sensitivity Rankings for Interior Modal Energies

Interior modal energy sensitivity frequency components to internal loss factor variations are calculated by using (3.14) on the elements of the existing full scale automobile model shown in Figure 3.2. The over car and under car volumes are not part of the vehicle design, their sensitivities are excluded. The sensitivity of the vehicle

INTERIOR's internal loss factor has the largest magnitude over all frequencies. This result arises from the diagonal element, N^{-1}_{KK}, which determines this sensitivity and confirms the diagonally dominant nature of N^{-1}(Hodges, et al 1987). Figure 3.2 also shows that the FLOORPAN, ENGCOMP and FOD have the next largest sensitivity values. This ranking indicates that these four design areas are the next most important to the acoustic performance of the vehicle. BODYPAN and HOOD have higher sensitivity than LRAIL and RRAIL over lower frequencies, however, have lower sensitivity over higher frequencies. Ranking all sensitivities of the interior SP to damping parameters of elements provides information as to the most effective direction for acoustic design changes. For the elements whose sensitivities have cross over these frequency ranges, one has to evaluate SP sensitivities in (3.6) for each of the parameters to determine which parameter has larger effect on the SP because one needs to evaluate both nodal energy sensitivity and the normalized SP spectrum α_j.

Table 3.1 Interior SP Sensitivities

ENGINE COMPARTMENT	LEFT RAIL	RIGHT RAIL	HOOD	BODY PANEL	FRONT of DASH	FLOOR PANEL	INTERIOR
0.356	1.92×10^{-2}	7.86×10^{-3}	1.39×10^{-2}	1.36×10^{-3}	0.337	0.640	0.954

The interior SP sensitivities over the full frequency range to element damping ratios and reverberation times are listed in Table 3.1. The table shows that the reverberation time in the interior has the maximum sensitivity and the second is the damping ratio in the floor panel and that the right frame rail and body panel have the least sensitivities. From viewpoint of design, the most efficient ways to reduce the noise levels in the vehicle interior from the engine surface vibration are to decrease the reverberation time in the interior by acoustic treatment and increase the damping ratio in the floor panel. The most inefficient ways are to increase the damping in the right frame rail and body

panels. The floor panel has the second greatest SP sensitivities and the acoustic treatment to the interior may be much expensive. Then increasing the floor panel damping to reduce interior SP may be chosen as a design alternative. SP sensitivities for front of dash and engine compartment are in the same order. This also gives design alternative to balance the cost effective in reducing vehicle interior noise.

3.6 Conclusions

Methodology developed in this paper extends traditional Statistical Energy Analysis beyond prediction of mean-rms vibro-acoustic response. The methodology uses SEA response sensitivity in each frequency band to derive SP sensitivity. SP sensitivity analysis relates the variability of SP to model design parameter variability in the SEA equations. This methodology is important for acoustic design of aircraft, ship and automotive vehicles because it enables users to qualitatively and quantitatively determine and rank the variations of vehicle interior SP with respect to changes of design parameters. The methodology identifies the most and least sensitive design parameters to SP in an SEA model. The methodology is powerful design tool for identifying the most effective areas for change in acoustic design.

Chapter 4 Putting Statistics into SEA*

4.1 Introduction

Statistical Energy Analysis (SEA) is of particular interest to the automotive industry because it can predict sound and vibration levels at higher frequencies than differential equation based analytical methods. SEA has been successfully employed by the aerospace industry (Lyon, R.H., 1975, Jacobs, E.W., et. al., 1989) and the maritime industry (Jenson, J.O., 1979) The analytical foundation of SEA is the concept that the vibration and sound energy of dynamic systems is shared equally between modes over narrow band of frequency (Lyon, R.H., 1975). For automotive vehicles, this concept makes SEA most accurate at frequencies above 300-500 Hz. where the number of modes in octave bands is high enough to allow averaging of the energy between the modes. As an example, a typical automotive interior has approximately 27 modes per Hz. at 5,000 Hz. Differential equation methods like the Finite Element Method have difficulty maintaining accuracy due to the same high modal density at these frequencies (Remington, P.J. and Manning, J.E., 1975, Lu, L.K.H., et. al., 1983).

Design of quality vehicles requires analytical methods that can accurately predict both the expected performance of designs and the variance of vehicle performance about the expected performance. Design analysis is needed for two purposes, the evaluation of existing vehicle designs and the development of specifications for new designs. Existing vehicle designs are evaluated to predict typical vehicle vibration and acoustic response

---

* The Chapter is based on the paper titled "Putting Statistics into The Statistical Energy Analysis of Automotive Vehicles" in Vibration Isolation, Acoustics and Damping in Mechanical Systems, DE-VOL 62 ASME Book G00823

and the probability that a vehicle will perform within specified performance specifications. During vehicle design development, subsystem specifications are used to develop predictions of expected system performance and variance. Both expected value and variance of SEA models are required to predict confidence levels in both classes of design analysis.

Current SEA modeling software provides RMS response predictions for such an SEA automotive vehicle model. Early SEA development by Lyons (1975) provided variance analysis for a few simple example systems and the response variance for randomly varying resonant frequencies was studied by DeJong (1985), however, no general approach to the variance analysis problem for design parameters is currently available in literature. The work discussed here extends SEA to include variance calculations.

4.2 SEA Response Variance Analysis

Response variance analysis gives the statistical distribution of predicted SEA energy levels about their mean values. Conventional SEA predicts the expected (RMS) values of SEA energies in the form of frequency spectra. Random distributions of physical parameter values lead to variance of predicted SEA energies about their expected frequency spectra values. These variances in SEA responses are implicitly, non-linearly, associated with variances of physical parameters via the SEA equation (1.1). This implicit variance relationship is derived through non linear definitions of the SEA parameters such as modal density, internal loss factor and coupling loss factor. SEA response statistics are dependent on the statistics of the model's physical parameters in these definitions. We will derive a linear approximate variance expression for SEA responses about mean-rms spectra in terms of physical parameters through a Taylor expansion.

The SEA response deviation about its mean-rms energy can be approximated by first order Taylor expansion over the M physical parameters and K SEA element inputs.

$$\Delta E_i = E_i - \bar{E}_i$$
$$= \sum_{m=1}^{M} \left.\frac{\partial E_i}{\partial x_m}\right|_{\substack{\mathbf{x}=\bar{\mathbf{x}} \\ \mathbf{P}=\bar{\mathbf{P}}}} \left[x_m - \bar{x}_m\right] + \sum_{k=1}^{K} \left.\frac{\partial E_i}{\partial P_k}\right|_{\substack{\mathbf{x}=\bar{\mathbf{x}} \\ \mathbf{P}=\bar{\mathbf{P}}}} \left[P_k - \bar{P}_k\right] \tag{4.1}$$

The partial derivatives of the i^{th} element's energy response above are evaluated at the nominal physical parameters $\mathbf{x} = \bar{\mathbf{x}}$ and nominal power inputs $\mathbf{P} = \bar{\mathbf{P}}$.

Taking the variance (Clifford, A.A., 1973, Oh, H.L., 1987) of (4.1) yields the variance of SEA responses, $\sigma^2(E_i)$, in terms of the variances of M physical parameters and K input powers.

$$\sigma^2(E_i) = \sum_{m=1}^{M} \left[\left.\frac{\partial E_i}{\partial x_m}\right|_{\substack{\mathbf{x}=\bar{\mathbf{x}} \\ \mathbf{P}=\bar{\mathbf{P}}}}\right]^2 \sigma^2(x_m) + \sum_{k=1}^{K} \left[\left.\frac{\partial E_i}{\partial P_k}\right|_{\substack{\mathbf{x}=\bar{\mathbf{x}} \\ \mathbf{P}=\bar{\mathbf{P}}}}\right]^2 \sigma^2(P_k) \tag{4.2}$$

where $\sigma^2(E_i)$ is the variance of total energy response in the i^{th} element,

$\sigma^2(x_m)$ is the variance of the m^{th} physical parameter, and

$\sigma^2(P_k)$ is the variance of the k^{th} power input

The SEA response derivatives are derived in Section 3.3.

4.3 Examples and Monte Carlo Validation

Two examples and a Monte Carlo modeling procedure are used here to validate the variance analysis. A set of two thousand (2,000) Gaussian distributed parameter values are first generated to simulate a production process. The mean and variances of these parameters are used in the variance analysis to predict the mean and variance of SEA response energies. The two thousand parameter values are then used in two thousand separate SEA analyses to compute 2,000 actual SEA responses. The mean and variance of these actual SEA responses are then compared with the variance analysis predictions of mean and variance.

The first example is a simple conceptual model (Figure 1.2) to illustrate the details of the analytical development and Monte Carlo test verification. This SEA model has the

topology similar to that shown in Figure 1.1. Acoustic power is input to the first cube and 5,000 Hz. is taken as the analysis band center frequency. In the variance analysis, the plate thickness h is chosen to be non stationary, $x_1 = h$ and we calculate the variance of total energy response in the second acoustic space, $\sigma(E_3)$. A Gaussian distribution of 2,000 plate thicknesses with mean value of 7.5×10^{-3} m and standard deviation of 5% of the mean, $\sigma(x_1) = 3.73 \times 10^{-4}$ (meters), is generated from a MATLAB software call. Note that the *actual* standard deviation of the data sample generated does not exactly equal the *requested* value for the sample. The histogram of 2,000 Gaussian distributed plate thicknesses is shown in Figure 4.1.

The variance of the second acoustic space response (4.2) is dependent only on the variance of the plate thickness because the variances of the input powers are zero.

$$\sigma^2(E_3) = \left[\left. \frac{\partial E_3}{\partial x_1} \right|_{\substack{x_1 = h \\ \mathbf{P} = \bar{\mathbf{P}}}} \right]^2 \sigma^2(x_1) \tag{4.3}$$

The derivative of total energy response with respect to x_1 includes only the first term in (3.7a) because modal density in the second acoustic space is independent of the plate thickness.

$$\frac{\partial E_i}{\partial x_1} = n_3 \frac{\partial e_3}{\partial x_1} \tag{4.4}$$

The derivative of the SEA coefficient matrix **N** with respect to plate thickness is needed in order to compute the derivative of modal response with respect to plate thickness. Since the plate thickness is associated only with the plate modal density, n_2, coupling loss factors η_{12} and η_{23} (3.9) includes only three terms.

$$\frac{\partial \mathbf{N}}{\partial x_1} = \frac{\partial \mathbf{N}}{\partial n_2}\frac{\partial n_2}{\partial x_1} + \frac{\partial \mathbf{N}}{\partial \eta_{12}}\frac{\partial \eta_{12}}{\partial x_1} + \frac{\partial \mathbf{N}}{\partial \eta_{23}}\frac{\partial \eta_{23}}{\partial x_1} \tag{4.5}$$

The terms, $\frac{\partial \mathbf{N}}{\partial n_2}$, $\frac{\partial \mathbf{N}}{\partial \eta_{12}}$ and $\frac{\partial \mathbf{N}}{\partial \eta_{23}}$, can be obtained by using (3.9). The derivatives with respect to $x_1 = h$ at 5,000 Hz of modal density n_2 , as well as coupling loss factors

η_{12} and η_{23} can be derived from their definitions (A1, Appendix A).

$$\frac{\partial n_2}{\partial x_1} = -\frac{\sqrt{3}A}{h^2 c_l} \tag{4.6}$$

$$\frac{\partial \eta_{23}}{\partial x_1} = -\frac{\rho_{AIR} C_{AIR}}{10000 \rho_{ALU} \pi h^2 \left(1 - \frac{1}{400h}\right)^{\frac{1}{2}}} \left(1 + \frac{1}{800h\left(1 - \frac{1}{400h}\right)}\right) \tag{4.7}$$

$$\frac{\partial \eta_{12}}{\partial x_1} = \frac{\partial}{\partial x_1}\left(\frac{n_2 \eta_{23}}{n_1}\right) = \frac{\partial n_2}{\partial x_1}\frac{\eta_{23}}{n_1} + \frac{n_2}{n_1}\frac{\partial \eta_{23}}{\partial x_1} \tag{4.8}$$

The above analysis gives $\left.\frac{\partial E_3}{\partial x_1}\right|_{\substack{x_1 = h \\ \mathbf{P} = \bar{\mathbf{P}}}} = 4.0 \times 10^{-4}$ and $\sigma(E_3) = 1.5 \times 10^{-7}$.

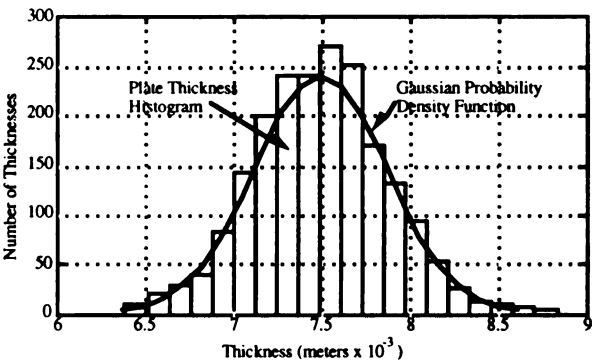

Figure 4.1 Plate Thickness Histogram and Corresponding Gaussian Probability Density

Monte Carlo verification of the above variance analysis is started by computing 2,000 SEA model responses from 2,000 separate models, one for each of the 2,000 thicknesses used in the SEA model. The standard deviation of the 2,000 values for total energy response in the second cube, E_3^{MC}, from the Monte Carlo test is $\sigma(E_3^{MC}) = 1.4 \times 10^{-7}$. The histogram for the 2,000 total energy responses computed for the second acoustic space is plotted in Figure 4.2 along with the predicted distribution

(solid line). In order to further compare the analytical results with the Monte Carlo results, mean value and variance for the actual model responses in the second acoustic space , E_3^{MC}, were used to plot the Gaussian probability density function (broken line) for the 2,000 model analyses.

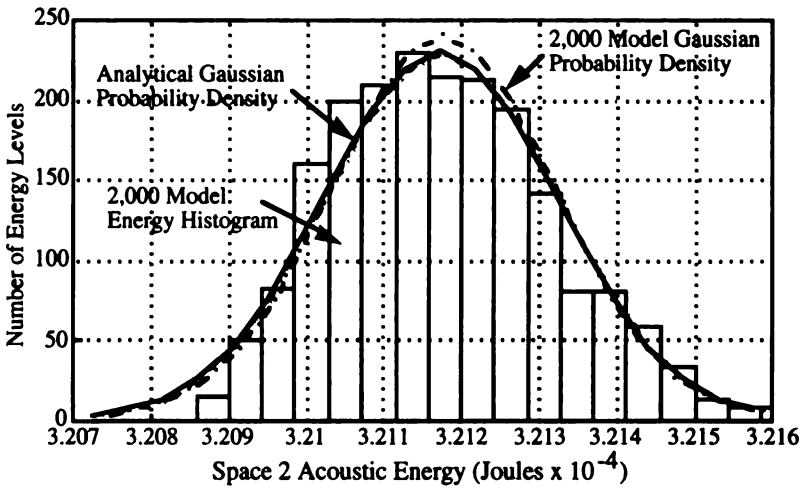

Figure 4.2 Gaussian Analytical Probability Density Function (PDF) Prediction for Acoustic Energy in Space #2 Compared with Histogram and PDF for 2,000 Model Monte Carlo Test Results

The variance analysis probability density function result (solid line) agrees very well with the probability density function computed for the 2,000 SEA model Monte Carlo test. The linear analytical standard deviation prediction has an error that is less than 5% of the actual standard deviation for the 2,000 models computed from Monte Carlo test results. This error can be partially attributed to the population of random physical parameter used in Monte Carlo tests. Figure 4.1 shows that the thickness population is not large enough (2,000 models) for the random generator used in the computation to approach a Gaussian distribution accurately. Increasing the number of models generated in the Monte Carlo tests would have required a prohibitive amount of computational effort. The remaining error can be attributed to the effects of non-linearities in the parameters on predicted variance and will be discussed in the second example.

The second example is an automotive vehicle SEA model (Figure 2.2 and 2.3). To demonstrate the variance analysis, the floor panel thickness is chosen to be non stationary and analysis of the vehicle interior sound level will be conducted at a band center frequency of 5,000 Hz. Two thousand (2,000) of the Gaussianly distributed floor panel thicknesses are generated with mean 7.50×10^{-4} (m) and 5% standard deviation 0.38×10^{-4}(m). The floor panel thickness histogram and associated ideal Gaussian probability density function are presented in Figure 4.3. The mean and variance of the

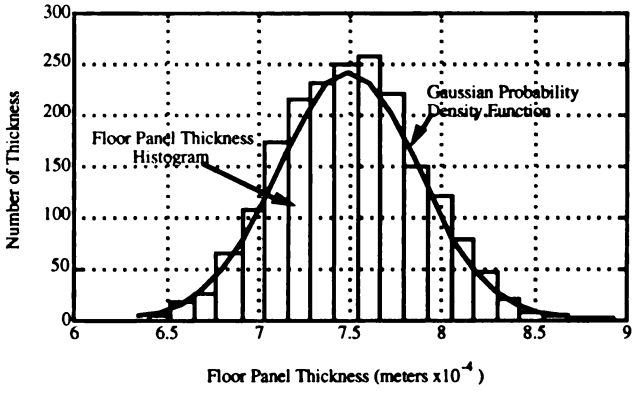

Figure 4.3 Floor Panel Thickness Histogram and Probability Density Function

floor panel data generated are then used in the variance analysis to compute predictions of mean and variance of the SEA energy responses. These predictions used formulas developed in this paper and evaluated the derivative of the interior total energy responses with respect to the floor panel thickness at the nominal system parameters. The predicted variance of the interior total energy response at 5,000 Hz. from floor panel thickness variance is 2.84×10^{-12} (Joules). After computing 2,000 of SEA total energy responses in the interior at 5,000 Hz by our Monte Carlo procedure, actual model interior acoustic energy responses were found to have a variance of 2.79×10^{-12} (Joules). The predicted and actual variance differ by less than 2%. The analytical variance prediction requires only about 1/300 of the computational effort (flops) of that required to compute the 2,000 models responses. The histogram of the interior total energy responses and the Gaussian

probability density functions from Monte Carlo test and analytical variance analysis at 5,000 Hz. are shown in the Figure 4.4. The results show that the linear variance approximations are effective to a complicated automotive vehicle SEA model.

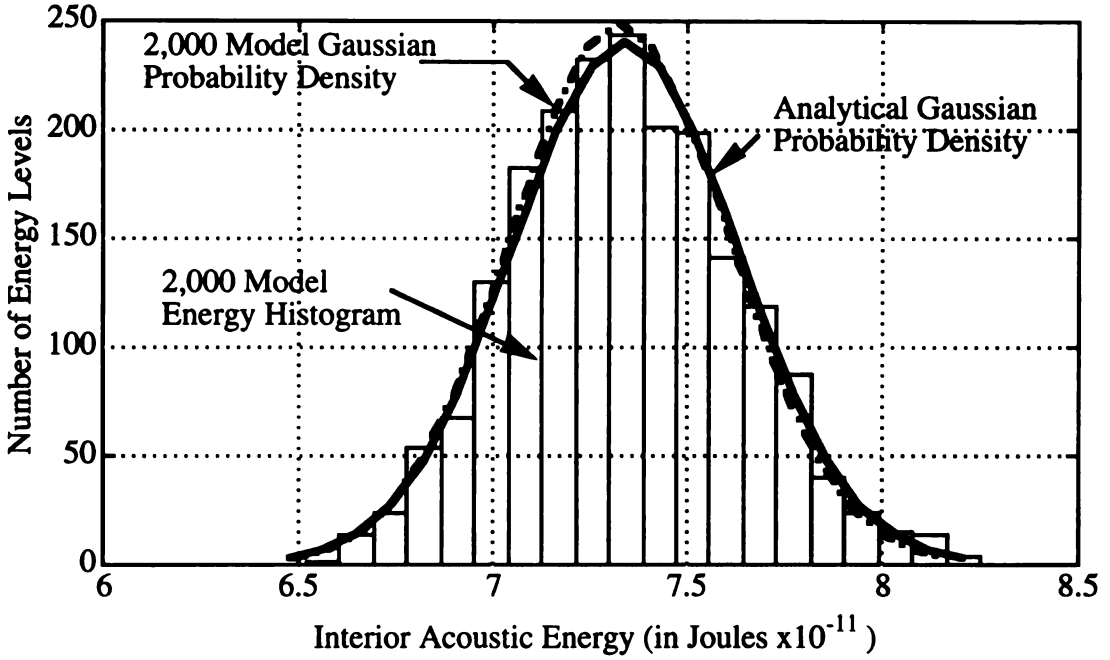

Figure 4.4 Histogram and Gaussian Probability Densities from Analytical and Monte Carlo Tests for Standard Deviation 5% of Floor Panel Thickness at 5,000 Hz.

The effect of nonlinearities in the SEA coefficient computations on the accuracy of the Taylor expansion was evaluated by running 8 different Monte Carlo validations for differing floor panel variances (of mean value). 2,000 of the physical parameter are generated from the Gaussian distributions for each of the standard deviation choices, 2,000 total interior energy responses (in Joules) are computed for each of the cases and the standard deviations for the responses are computed from Monte Carlo test runs and the analytical standard deviations from linear variance analysis are computed for each of the cases in Figure 4.5.

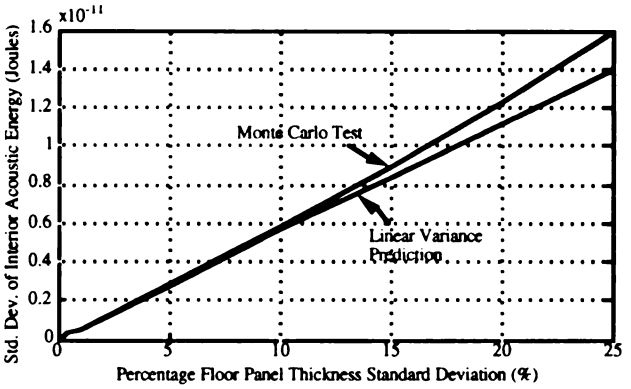

Figure 4.5 Comparison of Standard Deviations of Response Energy in the Vehicle Interior at 5,000 Hz. from Analytical Prediction and Monte Carlo Test due to Deviation in Floor Panel Thickness

The linear variance analysis prediction for a standard deviation of 15% of floor panel thickness has only a 6% error relative to the actual Monte Carlo test results which corresponds to only about 0.7% of the mean vehicle interior sound energy of 7.33×10^{-11} Joules computed for the models. Note that a 5-15% floor panel thickness standard deviation may well be greater than acceptable in any actual production process and is used here for discussion purposes only. The variance linear approximation is quite effective and robust to physical parameter variations.

4.4 Conclusions

The analytical variance theory put forth in this paper can accurately predict the SEA model response statistics, the linear approximation is shown to be robust over a broad range of the physical parameter variations tested and the effectiveness of the analytical algorithm is validated by two examples. The algorithm can be applied to evaluate the robustness of existing vehicle designs to variations of design parameters and to develop specifications for new designs. In particular the algorithm can also be used in the early design stages for a prototype. The accurately predicted variances of SEA model with expected values can be used to predict confidence levels in the design analyses.

With those features and applications, the variance theory on SEA vibro-acoustic responses provides a powerful design tool for quality automotive vehicle designs. Designers can acquire quantitative information on the relationship between the design SEA responses and the design physical parameters affecting the mean-rms performance and the variability in the design performance caused by the variability in the design physical parameters. This will allow designers to develop specifications to achieve optimal and/or ultimate robust designs.

Chapter 5 Probability Distribution of SEA Responses*

5.1 Introduction

Quality acoustic designs for aircraft, ships, and automotive vehicles require the probability analysis of extreme vibro-acoustic response values. Probability distributions of SEA responses determine the response variances and confidence levels needed to evaluate the probability of excessive acoustic noise and structural vibration (Lyon, 1987). Study of variance and confidence level of SEA responses was initiated by Lyon (1967, 1975, 1987). In his study, Gamma response distributions were chosen to compute confidence levels because they have the desirable feature of strictly positive values. SEA response variance analysis for automotive vehicle was investigated by DeJong (1985). An exceptionally large experimental study (156 production cars) of vibro-acoustic response statistics was conducted by Kompella and Bernhard (1993).

SEA response distributions in frequency bands are proven to be Gaussian for infinite number of design parameters in this work. Sound and velocity are directly proportional to SEA responses, their distributions are also proven to be Gaussian. In engineering applications, the number of design parameters is always finite for SEA models. A Monte Carlo test and a Statistical Hypothesis test on a simple 3 element SEA model show that Gaussian distributions are good approximations for responses of an SEA model with a finite number of design parameters.

---

* This Chapter is based on the paper with the same title to be submitted to Journal of Vibration and Acoustics.

5.2 Statistical Distribution of SEA Responses

Distributions of SEA responses originate from randomness of design parameters. The design parameters have arbitrary distributions. The design parameters are used to compute SEA responses and the randomness from the design parameters passes to the SEA responses through SEA equations. The SEA response randomness is characterized by SEA response distribution. The SEA response distributions can be used for vibro-acoustic design purposes by computing probability of excessive vibro-acoustic response and response confidence levels.

The Gaussian distribution derivations for SEA responses have been done by the following steps. Step 1 makes all necessary assumptions. Step 2 expands SEA responses by Taylor expansions. Step 3 shows Lyapunov condition in The Central Limit Theorem for SEA responses is satisfied under these assumptions. Step 4 checks these assumptions in Step 1 for SEA responses and points out situations for both holding and violating these assumptions.

Step 1: Assumptions. (1): SEA response derivatives with respect to SEA parameters and SEA parameter derivatives to design parameters are bounded above. (2): Third order absolute moments of all design parameters are bounded above. (3): there is no single statistically dominant variable.

Step 2: SEA Expansions. The SEA responses are non-linearly and implicitly related to design parameters. The probability distribution derivation of SEA responses requires SEA response for the i^{th} element at a single frequency, f_k, be linearly and explicitly expressed in terms of design parameters by Taylor Expansions.

$$\begin{aligned} E_{i,k} &\approx \overline{E}_{i,k} + \sum_{m=1}^{N_x} \left.\frac{\partial E_{i,k}}{\partial x_m}\right|_{\substack{\mathbf{x}=\overline{\mathbf{x}} \\ \mathbf{P}=\overline{\mathbf{P}}}} \left(x_m - \overline{x}_m\right) \\ &\approx \overline{E}_{i,k} + \sum_{m=1}^{N_x} \left(y_m - \overline{y}_m\right) \end{aligned} \tag{5.1}$$

where $\overline{E}_{i,k}$ is SEA response expected value evaluated at nominal parameters

N_x is the number of design parameters.

$\frac{\partial E_{i,k}}{\partial x_m}$ is SEA response derivatives with respect to design parameters

$$y_m = \left.\frac{\partial E_{i,k}}{\partial x_m}\right|_{\substack{\mathbf{x}=\bar{\mathbf{x}} \\ \mathbf{P}=\bar{\mathbf{P}}}} x_m \text{ and } \bar{y}_m = \left.\frac{\partial E_{i,k}}{\partial x_m}\right|_{\substack{\mathbf{x}=\bar{\mathbf{x}} \\ \mathbf{P}=\bar{\mathbf{P}}}} \bar{x}_m$$

The partial derivatives above are evaluated at the nominal design parameters $\mathbf{x} = \bar{\mathbf{x}}$ and nominal power inputs $\mathbf{P} = \bar{\mathbf{P}}$.

Step 3: The Central Limit Theorem (CLT) and Lyapunov Condition. CLT can be invoked to derive the distributions of SEA energy responses which are sums consisting of a number of independent random variables with arbitrary distributions (5.1). The CLT states (Cramér, pg 215, 1963): let $y_1, y_2, \ldots, y_n$ be independent variables with arbitrary distributions, finite expected values, and variances $\sigma^2(y_i)$. If a Lyapunov Condition:

$$\omega_n = \sqrt[3]{\sum_{m=1}^{n} M_3\left(|y_m - \bar{y}_m|\right)} \Big/ \sqrt{\sum_{m=1}^{n} \sigma^2(y_m)} \to 0 \ \ as \ \ n \to \infty \tag{5.2}$$

where $M_3\left(|y_m - \bar{y}_m|\right)$ is the third order absolute central moment of y_m and

n is the number of the variables

is satisfied, the random variable, $z = \sum_{i=1}^{n} y_i \Big/ \sqrt{\sum_{i=1}^{n} \sigma^2(y_i)}$ tends asymptotically to a Gaussian distribution.

The third order absolute moment $M_3\left(|y_m - \bar{y}_m|\right)$ and variance $\sigma^2(y_m)$ of intermediate variable y_m about its mean $\bar{y}_m$ in (5.1) are needed to check the Lyapunov condition for SEA responses. The third order absolute central moment of y_m for SEA responses can be expressed in terms of the third order absolute moments of x_m about its mean $\bar{x}_m$ using the linearity property of the moments.

$$M_3\left(|y_m - \bar{y}_m|\right) = \left[\left.\frac{\partial E_{i,k}}{\partial x_m}\right|_{\substack{\mathbf{x}=\bar{\mathbf{x}} \\ \mathbf{P}=\bar{\mathbf{P}}}}\right]^3 M_3\left(|x_m - \bar{x}_m|\right) \tag{5.3}$$

The variance $\sigma^2(y_m)$ of y_m can be expressed in terms of variance $\sigma^2(x_m)$ of x_m.

$$\sigma^2(y_m) = \left[\left. \frac{\partial E_{i,k}}{\partial x_m} \right|_{\substack{\mathbf{x}=\bar{\mathbf{x}} \\ \mathbf{P}=\bar{\mathbf{P}}}} \right]^2 \sigma^2(x_m) \tag{5.4}$$

The Lyapunov Condition for SEA energy responses can be obtained by substituting (5.3) and (5.4) into (5.2).

$$\omega_{N_x} = \sqrt[3]{\sum_{m=1}^{N_x} \left[\left. \frac{\partial E_{i,k}}{\partial x_m} \right|_{\substack{\mathbf{x}=\bar{\mathbf{x}} \\ \mathbf{P}=\bar{\mathbf{P}}}} \right]^3 M_3\left(|x_m - \bar{x}_m|\right)} \Bigg/ \sqrt{\sum_{m=1}^{N_x} \left[\left. \frac{\partial E_{i,k}}{\partial x_m} \right|_{\substack{\mathbf{x}=\bar{\mathbf{x}} \\ \mathbf{P}=\bar{\mathbf{P}}}} \right]^2 \sigma^2(x_m)} \tag{5.5}$$

where N_x is the number of random design parameters in SEA model

If the upper bound of ω_{N_x} in (5.5) approaches zero as N_x goes to infinity, (5.5) will satisfy the Lyapunov Condition (5.2) for SEA energy responses. The Lyapunov Condition (5.5) is determined by three quantities, SEA response derivatives, $\partial E_{i,k}/\partial x_m$, design parameter third order absolute central moments $M_3\left(|x_m - \bar{x}_m|\right)$ and variances, $\sigma^2(x_m)$. The absolute values of SEA response derivatives under assumption (1) are bounded above and therefore have a maximal value.

$$\max\left\{ \frac{\partial E_{i,k}}{\partial \mathbf{x}} \right\} = \max\left\{ \left| \left. \frac{\partial E_{i,k}}{\partial x_m} \right|_{\substack{\mathbf{x}=\bar{\mathbf{x}} \\ \mathbf{P}=\bar{\mathbf{P}}}} \right|, \ m = 1,2,\cdots,N_x \right\} \tag{5.6}$$

The absolute values of SEA response derivatives under assumption (1) are bounded below away from zero and have a minimal value obtained by ignoring the trivial case of zero-SEA parameter derivatives.

$$0 < \min\left\{ \frac{\partial E_{i,k}}{\partial \mathbf{x}} \right\} = \min\left\{ \left| \left. \frac{\partial E_{i,k}}{\partial x_m} \right|_{\substack{\mathbf{x}=\bar{\mathbf{x}} \\ \mathbf{P}=\bar{\mathbf{P}}}} \right|, \ m = 1,2,\cdots,N_x \right\} \tag{5.7}$$

An upper bound for the Lyapunov Condition (5.5) can be obtained by replacing the derivatives in the numerator with the maximal value and replacing the derivatives in the denominator with the minimal value.

$$\begin{aligned}\omega_{N_x} &\le \max\left\{\frac{\partial E_{i,k}}{m\partial \mathbf{x}}\right\}\sqrt[3]{\sum_{m=1}^{N_x} M_3\left(\left|x_m-\bar{x}_m\right|\right)}\Big/\min\left\{\frac{\partial E_{i,k}}{\partial \mathbf{x}}\right\}\sqrt{\sum_{m=1}^{N_x}\sigma^2(x_m)} \\ &= C_{mm}\sqrt[3]{\sum_{m=1}^{N_x} M_3\left(\left|x_m-\bar{x}_m\right|\right)}\Big/\sqrt{\sum_{m=1}^{N_x}\sigma^2(x_m)} \\ \text{where } C_{mm} &= \max\left\{\frac{\partial E_{i,k}}{\partial \mathbf{x}}\right\}\Big/\min\left\{\frac{\partial E_{i,k}}{\partial \mathbf{x}}\right\}\end{aligned} \tag{5.8}$$

The bounds of the variances and moments can be used to further simplify the upper bound of ω_{N_x} (5.8). The third order absolute moments of design parameters, $M_3\left(\left|x_m-\bar{x}_m\right|\right)$, are bounded above under assumption (2). Therefore the third absolute central moments have a maximal value. Zero variance variables are not random hence the zero-variance variables can be excluded from the moment and variance calculation. For random variables, the variances are bounded below away from zero and have a non-zero minimal value. The upper bound for the Lyapunov Condition (5.8) can be simplified by replacing the summation for the third absolute central moments in the numerator with the product of the moment maximal value and the number of the design parameters. The summation for the variances in the denominator is replaced with the product of the non-zero variance minimal value and the number of the design parameters.

$$\begin{aligned}\omega_{N_x} &\le C_{mm}\sqrt[3]{\max_m\left\{M_3\left(\left|x_m-\bar{x}_m\right|\right)\right\}N_x}\Big/\sqrt{\min_m\left\{\sigma^2(x_m)\right\}N_x} \\ &= D_{mm}/\sqrt[6]{N_x} \\ \text{where } D_{mm} &= C_{mm}\sqrt[3]{\max_m\left\{M_3\left(\left|x_m-\bar{x}_m\right|\right)\right\}}\Big/\sqrt{\min_m\left\{\sigma^2(x_m)\right\}}\end{aligned} \tag{5.9}$$

The Lyapunov Condition for SEA energy response in (5.9) has a constant D_{mm} in the numerator and N_x in the denominator. Letting N_x go to infinity, the constant term in the numerator remains unchanged and the denominator, $\sqrt[6]{N_x}$, goes to infinity, so The Lyapunov Condition, $\omega_{N_x} \to 0$. The Lyapunov condition is satisfied which guarantees that probability distributions of SEA responses, $E_{i,k}$, tend asymptotically to Gaussian distributions with a mean of $\overline{E}_{i,k}$ and a variance of $\sum_{m=1}^{N_x}\left[\left[\frac{\partial E_{i,k}}{\partial x_m}\right|_{\substack{\mathbf{x}=\bar{\mathbf{x}}\\ \mathbf{P}=\bar{\mathbf{P}}}}\right]\right]^2\sigma^2(x_m)$.

Step 4: Assumption Check on SEA Response Derivatives. The SEA modal response derivatives with respect to SEA parameters, $\partial e_{i,k}/\partial x_m$, in the first term in (3.7a) are the product of three terms: $\mathbf{N}^{-1}$, $\partial \mathbf{N}/\partial x_m$ ($x_m = n_i, \eta_i$ *and* η_{ij}) and $\mathbf{e}$ (3.8). For a strongly connected SEA model, $\mathbf{N}$ is positive definite, diagonally dominant and $\mathbf{N}^{-1}$ exists and is diagonally dominant (Hodges, et al, 1987, Huang and Radcliffe, 1993). All entries in $\mathbf{N}$ are linear combinations of modal densities, internal loss factors and coupling loss factors. These entries are finite for finite frequencies. The entries in $\mathbf{N}$ are bounded by their diagonal entries and so are the entries in $\mathbf{N}^{-1}$. The entries in the derivatives are sparse and functions of modal densities, internal loss factors and coupling loss factors (3.9). For this reason, the entries in $\partial \mathbf{N}/\partial x_m$ are bounded for finite frequencies. The modal energy response, $\mathbf{e}$, is associated linearly to power inputs which drive the systems. The modal energy response, $\mathbf{e}$, is bounded over finite frequency bands for bounded power inputs. The modal density derivatives with respect to SEA parameters are either 1 or zero. Therefore, the SEA response derivatives with respect to SEA parameters in (3.7a) are bounded.

Most SEA parameter derivatives with respect to design parameters exist and are continuous in a closed interval in which the design parameters are defined and hence bounded. Some SEA parameters, such as structural-acoustic coupling loss factor (Lyon, 1975), have jumps at a critical frequency and their derivative at that critical frequency does not exist, however, the right-side and left-side derivatives exist and are bounded. The analysis frequency band can be divided into two closed sub-intervals separated by the critical frequency. The SEA parameter derivatives are continuous in the closed sub-intervals and hence are bounded. One can conclude in general that SEA parameter derivatives with respect to design parameters are piece-wise continuous in closed intervals and bounded. Although bounds do not exist at critical frequencies, SEA response derivatives are bounded in piece-wise closed intervals for finite frequencies.

Assumption (2) sets an upper bound for the third order absolute moments of design

parameters. The larger the upper bound the slower the Lyapunov Condition goes to zero. This feature has significance in engineering applications. There is never an infinite number of design parameters in any SEA engineering models. Gaussian distributions derived here are only an approximation for SEA responses in engineering applications. Small third order absolute moments mean small deviations among design parameters. Small deviations from nominal design parameters will lead to good approximations to Gaussian distributions. In other words, for small third order absolute moment upper bounds, only a small number of random design parameters are needed to achieve good approximations to Gaussian distributions. Assumption (3) guarantees that no single random design parameter, x_m, in (5.1) is statistically dominant. Otherwise, the SEA response distributions will follow the distribution of the dominant random variable in (5.1).

5.3 Distribution of Total Pressure and Velocity

Distributions of total mean squared (ms) pressure and velocity, p_i^2 and v_i^2 in (1.5), will have a normal distribution if the ms pressure and velocity frequency components $p_{i,k}^2$ and $v_{i,k}^2$ have a normal distribution because the total pressure and velocity are linear combinations of independent pressure and velocity frequency components, $p_{i,k}^2$ and $v_{i,k}^2$,. The ms pressure and velocity frequency components are linearly associated with SEA energy responses (1.4). The method used to derive the approximate distribution of SEA energy responses in the previous section can be used to derive the distributions of the ms sound pressure and velocity.

The distributions of the ms pressure and velocity frequency components require the linear approximation of the ms pressure and velocity frequency components in terms of the random design parameters. Taking the structural velocity frequency response component as an example, , and assuming the first design parameter $x_1 = m_i$, the element mass, the second equation in (1.4) can be written as:

$$v_{i,k}^2(f_k,\mathbf{x}) = \frac{E_{i,k}}{x_1} \tag{5.10}$$

The Taylor expansion on (5.10) yields an approximation to the ms velocity.

$$v_{i,k}^2(f_k,\mathbf{x}) \approx \bar{v}_{i,k}^2(f_k,\mathbf{x}) + \left[\frac{1}{x_1}\sum_{m=1}^{N_x}\frac{\partial E_{i,k}}{\partial x_m}\right]\Bigg|_{\substack{\mathbf{x}=\bar{\mathbf{x}}\\ \mathbf{P}=\bar{\mathbf{P}}}}\left[x_m-\bar{x}_m\right] - \left[\frac{E_{i,k}}{x_1^2}\right]\Bigg|_{\substack{\mathbf{x}=\bar{\mathbf{x}}\\ \mathbf{P}=\bar{\mathbf{P}}}}\left[x_1-\bar{x}_1\right] \tag{5.11}$$

Comparing the ms velocity derivatives (5.11) to the SEA energy response derivatives (5.1), one finds that the ms velocity derivatives (5.11) can be obtained by dividing the SEA energy response derivatives (5.1) by a factor of $\bar{x}_1$, the nominal mass of the structural element, and subtracting a term, $\left.\frac{E_{i,k}}{x_1^2}\right|_{\substack{\mathbf{x}=\bar{\mathbf{x}}\\ \mathbf{P}=\bar{\mathbf{P}}}}\left[x_1-\bar{x}_1\right]$, from the SEA energy response derivative with respect to $x_1 = m_i$. Both the factor and the additional term are bounded. Therefore the derivatives of the ms structural velocity are bounded above and below away from zero. The assumptions on the variances and the third order absolute central moments of $\mathbf{x}$ are the same. The conclusions drawn from the bounded derivatives, variances and moments on $\mathbf{x}$ from the previous section can be applied to (5.11). One can conclude that the ms velocity frequency components, $v_{i,k}^2$, have Gaussian distributions. The same argument can also be applied to the ms pressure frequency components and they also have Gaussian distributions as the number of design parameters go to infinity.

The distributions of the ms pressure and velocity integrated over all frequencies are also Gaussian because they are the linear combinations of the ms pressure and velocity frequency components. The linear combination of Gaussian distributions of ms pressure and velocity frequency components yield Gaussian distributions for ms pressure and velocity.

5.4 Monte Carlo Test

Monte Carlo analysis of a simple model (Figure 1.1 and 1.2) is used here to test the theoretical results. The Gaussian distributions are only approximations for SEA responses distributions. The reasons are that the Lyapunov Condition for SEA responses in

engineering applications will not be zero because there will never be a infinite number of design parameters in any practical SEA model. The Lyapunov Condition is close to zero for large numbers of design parameters in an SEA model and this feature will be demonstrated in an SEA model example.

The SEA model example has 18 design parameters and 1 power input. Power inputs are set inversely proportional to band center frequency: $P_i = f_i^{-1.5} \times 10^{-4}$ Watts. Formulas used to calculate SEA parameters are from Lyon (Appendix A). Geometric parameters (Table A1, Appendix A), such as lengths and thicknesses are assumed to have Gaussian distributions with design values as means and 5% of the design values as their standard deviations. All other parameters, such as mass densities, speeds of sound, reverberation times, damping ratio, and input powers et al, are assumed to have uniform distributions in intervals of ±10% from their nominal values (see Appendix A). Third octave Band center frequencies range from 125 Hz. to 10,000 Hz. in 20 bands. 2,000 SEA models for each band are generated from these distributions and 2,000 total mean-squared acoustic pressures and structural velocities are computed from the SEA response statistics. The statistical population of SEA responses is used to verify the hypothetical Gaussian distributions and analytical standard deviation computations of SEA responses.

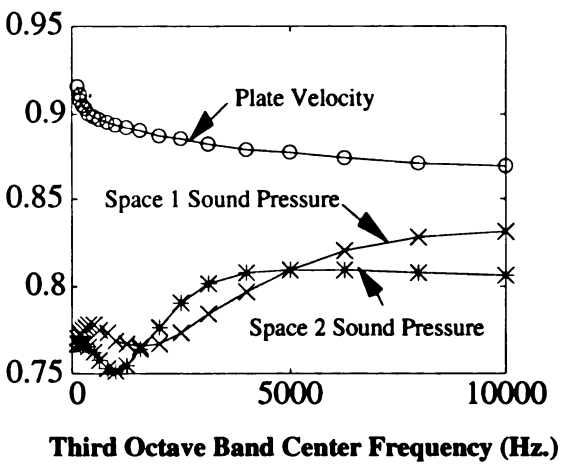

Figure 5.1 Lyapunov Condition Terms for SEA Responses

The Lyapunov Condition terms for each analysis band are shown in Figure 5.1. The maximum Lyapunov Condition terms are 0.832 at 10,000 Hz for space 1 sound pressure, 0.810 at 5,000 Hz. for space 2 sound pressure and 0.916 at 125 Hz for plate velocity in Figure 5.1. The Lyapunov Condition terms are non-zero for the finite number of random design parameters in contrast with the theoretical infinite order analysis. The finite order Lyapunov Condition terms are close to zero and the distribution from Monte Carlo test will be approximately Gaussian because of (1) the finite number of design parameters, $N_x = 19$, in the SEA model, (2) the finite number, $N_{mc} = 2{,}000$, of Monte Carlo tests. Note that the Figure 5.1 shows that the Lyapunov Condition terms for structural plate are

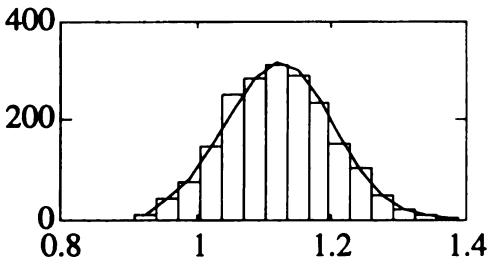

Figure 5.2 Space 1 ms Sound Pressure @ 1,000 Hz. Histogram ($\times 10^{-4} Pa^2$)

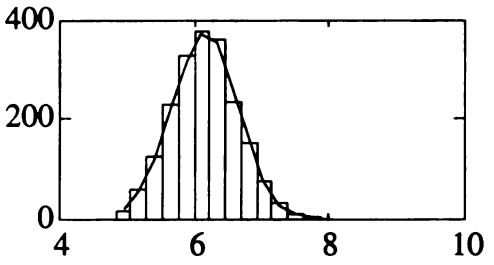

Figure 5.3 Space 1 Total ms Sound Pressure Histogram ($\times 10^{-3} Pa^2$)

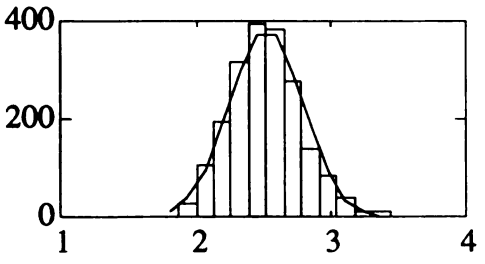

Figure 5.4 Plate ms Velocity @ 1,000 Hz. Histogram ($\times 10^{-4} mm^2 / sec^2$)

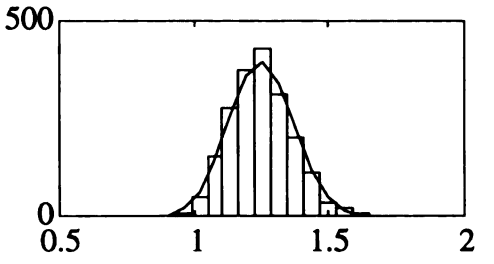

Figure 5.5 Plate Total ms Velocity Histogram($\times 10^{-1} mm^2 / sec^2$)

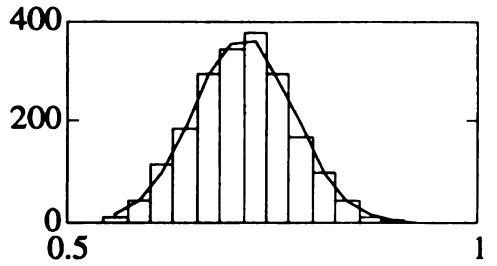

Figure 5.6 Space 2 ms Sound Pressure @ 1,000 Hz. Histogram ($\times 10^{-4}$ Pa^2)

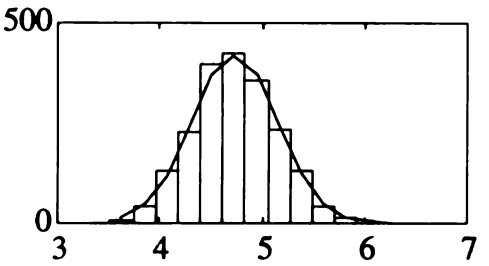

Figure 5.7 Space 2 Total ms Sound Pressure Histogram ($\times 10^{-3}$ Pa^2)

always larger than those for acoustic spaces. One can expect that the test data for spaces closer to Gaussian distribution than those of the plate.

Histograms for ms acoustic pressure at 1,000 Hz and total ms acoustic pressure and velocity for spaces and structural velocity for the plate are shown in Figures 5.2 to 5.7. The bars represent the histograms from Monte Carlo test runs and the solid lines represent the hypothetical Gaussian distribution with estimated means and standard deviation from the Monte Carlo samples. The histograms show that the mean-squared acoustic sound pressure and structural velocity distributions are well approximated by Gaussian.

5.5 Hypothesis Test

A Hypothesis test is used to examine the agreement between hypothetical Gaussian distributions and distributions from the Monte Carlo tests of the SEA model. The objective of the test is to find if deviations of hypothetical distributions from sample distributions are small enough to accept the hypothesis. The deviation is quantified by the normalized ms difference between cumulative frequency from the sample and from the hypothesis. χ^2 will be zero if the samples come from the true hypothesis distribution.

$$\chi^2 = \sum_{i=1}^{R} \left(F_i - N_{mc} P(A_i)\right)^2 / N_{mc} P(A_i) \tag{5.12}$$

where N_{mc} is the number of tests

A_i is a non-overlapping data interval

$P(A_i)$ hypothetical probability that data fall into the internal A_i

F_i is the number of data falling into A_i from Monte Carlo test and

R is the number of interval A_i

The χ^2 hypothesis test was introduced by Pearson (Cramér, 1963) who shown that, when N_{mc} is large enough, statistical quantity χ^2 obeys χ^2-distribution of degree of freedom $R-r-1$ (r is the number of parameters estimated from the sample). Let χ^2_α denote the $\alpha\%$ value of χ^2-distribution for degree of freedom $R-1$. The probability $P = P(\chi^2 > \chi^2_\alpha)$ will, for large N_{mc}, be approximately equal to $\alpha\%$. The probability is explained in two ways. First, if the value $\chi^2 > \chi^2_\alpha$ is found, the samples show a significant deviation from a hypothesis and the hypothesis shall be rejected at least until further experience had made it plausible that the deviation was due to random fluctuations. Second, the probability that the hypothesis is actually true and is falsely rejected is precisely the probability $P = P(\chi^2 > \chi^2_\alpha)$. On the other hand, if value $\chi^2 \le \chi^2_\alpha$ is found, then distribution from Monte Carlo test samples has no significant deviation from the hypothetical distribution and the hypothesis is accepted at the significant level α.

Hypothesis that SEA model response distributions are Gaussian is verified from the χ^2 hypothesis test. The frequency F_i and response data interval A_i are determined by the Monte Carlo test histogram results of SEA responses. The median x_i of the interval A_i and the frequency F_i are used to estimate the mean and standard deviations of the hypothetical Gaussian distribution by the maximum likelihood method. The estimated expected mean and standard deviation are used to evaluate the Gaussian distribution and to compute the probability $P(A_i)$.

A typical test result for total ms sound pressure in Space 2 is listed in Table 5.1. 2,000 (N_{mc} = 2,000) total ms sound pressure in space 2 from Monte Carlo test are divided into 15 intervals A_i. in the second column. The mean and standard deviation for the ms sound pressure are estimated from the medians x_i of intervals A_i in the second column

and the observed frequency in the fifth column in Table 5.1.

$$\begin{cases} \bar{\mu} = \dfrac{1}{2{,}000}\sum_{i=1}^{15} F_i x_i = 4.909\times 10^{-3}\ (\mathrm{P_a^2}) \\ \bar{s} = \sqrt{\dfrac{1}{2{,}000}\left(\sum_{i=1}^{15}\left(F_i x_i^2\right) - 2{,}000\bar{\mu}\right)} = 4.257\times 10^{-4} \end{cases} \tag{5.13}$$

The estimated mean and standard deviation are used to compute hypothetical probability $P(A_i)$ and hypothetical frequency , $N_{mc}P(A_i)$, in the fourth column in Table 5.1. Since Pearson Theorem is derived under the assumption that N_{mc} is large enough and $N_{mc}P(A_i)$ should not be small (in general $N_{mc}P(A_i)$ should be larger than 10), the 11^{th} to 15^{th} row in the fourth and fifth columns are combined to form the eleventh row in the sixth and seventh column. The combined hypothetical and observed frequencies in the sixth and seventh column are used to compute the contributions in each interval, A_i , to the χ^2 in

Table 5.1 χ^2-Test for Space 2 Total ms Sound Pressure

interval number	response interval A_i ($\times 10^{-3}$)	probability $P(A_i)$	hypothetical $N_{mc}P(A_i)$	observed F_i	hypothetical (combined)	observed (combined)	contribution to χ^2
1	3.654-3.880	0.006171	12.342	7	12.34	7	2.312
2	3.880-4.107	0.02229	44.58	44	44.58	44	0.007546
3	4.107-4.334	0.05846	116.92	122	116.9	122	0.2207
4	4.334-4.561	0.1176	235.18	231	235.2	231	0.07429
5	4.561-4.787	0.1798	359.6	387	359.6	387	2.088
6	4.787-5.014	0.2128	425.6	419	425.6	419	0.1023
7	5.014-5.241	0.1836	367.2	363	367.2	363	0.04804
8	5.241-5.468	0.1226	245.2	235	245.2	235	0.4243
9	5.468-5.694	0.06222	124.44	129	124.4	129	0.1671
10	5.694-5.921	0.02422	48.448	45	48.45	45	0.2454
11	5.921-6.148	0.006849	13.698	14	17.31	18	0.02739
12	6.148-6.375	0.001516	3.0322	1			
13	6.3750-6.602	0.0002564	0.51288	1			
14	6.602-6.828	3.1219E-05	0.062438	1			
15	6.828-7.055	2.9391E-06	0.0058782	1			
sum		0.9984	1997	2000			5.717

the last column. The normalized difference χ^2 is the summation of all rows in the last column, $\chi^2 = 5.717$. There are $R = 11$ intervals after combination and r=2 parameters estimated. The degree of freedom for the χ^2 distribution is $R - r - 1$=11-2-1=8. Tabulated values (Cramér, 1963) gives $\chi^2_{0.5} = 7.344 > \chi^2 = 5.717$. The inequality indicates that the hypothesis is accepted at significant level 50%.

Table 5.2 Hypothesis Test Result Summary for Spaces

	Space 1			Space 2		
	χ^2	$\chi^2_\alpha\ (d.o.f)$	α	χ^2	$\chi^2_\alpha\ (d.o.f)$	α
500 Hz.	7.297	7.584 (11)	0.75	5.709	8.383 (7)	0.3
1,000 Hz.	9.894	12.55 (10)	0.25	7.855	8.343 (9)	0.5
5,000 Hz.	9.268	9.342 (10)	0.5	8.493	10.66 (9)	0.3
Total ms SP (20 band)	6.784	8.343 (9)	0.5	5.717	7.344 (8)	0.5

The hypothesis test result for spaces is summarized in Table 5.2. The results show that the hypothesis that ms sound pressures in frequency bands and ms sound pressures obey Gaussian distribution is accepted.

A typical hypothesis test for total ms structural velocity of the plate, composed by 20 frequency bands, is listed in Table 5.3. The computation procedure and table contents are the same as Table 5.1. The normalized difference $\chi^2 = 43.33$ and the hypothesis should be rejected. However detailed examination of the contribution shows that the main contributors to χ^2 (60%) come from the first and last row. In other words, these contributions come from the neighborhood of 3-σ region. This phenomenon can be illustrated by plotting the cumulative percent frequency of the total ms velocity of the plate on a normal probability paper (Figure 5.8). The normal probability paper is designed such that all cumulative percent frequency points from a normal distribution lie in a straight line(Volk, 1969). The horizontal axis in Figure 5.8 is the response intervals, the vertical axis is the cumulative percent frequency and the straight line is determined by two

points: 50% at mean value and 84.13%. It can be seen from Figure 5.8 that most cumulative percent frequency points are close to the straight line and the points near two edge sides are farther from the straight line than other points. Overall the total ms velocity of the plate can be considered to have a Gaussian distribution. Therefore it is reasonable to exclude the contributions from the first and last row without causing large errors and compute $\chi^2 = 18.22$.

Table 5.3 χ^2-Test for Total ms Structural Velocity of the Plate

interval number	response interval ($\times 10^{-7}$)	probability $P(A_i)$	hypothetical $N_{mc}P(A_i)$	observed F_i	hypothetical (combined)	observed (combined)	contribution to χ^2
1	0.870-0.929	0.002778	5.560	1			
2	0.929-0.989	0.01043	20.87	10	26.43	11	9.005
3	0.989-1.029	0.03067	61.34	51	61.34	51	1.743
4	1.049-1.108	0.07053	141.1	154	141.1	154	1.187
5	1.108-1.168	0.1269	253.8	274	253.8	274	1.608
6	1.168-1.228	0.1787	357.4	376	357.4	376	0.9680
7	1.228-1.288	0.1972	394.4	430	394.4	430	3.213
8	1.288-1.347	0.1702	340.4	308	340.4	308	3.084
9	1.347-1.407	0.1151	230.2	202	230.2	202	3.455
10	1.497-1.467	0.06087	121.7	115	121.7	115	0.3732
11	1.467-1.526	0.02521	50.42	39	50.42	39	2.587
12	1.526-1.586	0.008165	16.33	25	21.42	40	16.11
13	1.586-1.646	0.002072	4.143	9			
14	1.646-1.705	0.0004111	0.8221	3			
15	1.705-1.765	6.381E-05	0.1276	3			
sum		0.9993	1999	2000			43.33

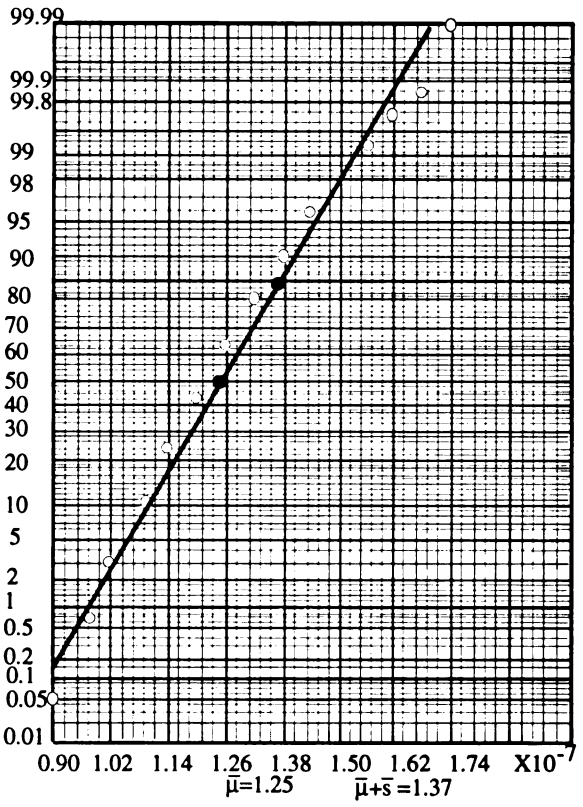

Figure 5.8 Normal Cumulative Graph of Total ms Velocity of Plate

Table 5.4 χ^2 Test for Structural Velocity of The Plate

	plate		
	χ^2	χ^2_α $(d.o.f)$	α
500 Hz.	16.42	16.81 (6)	0.01
1,000 Hz.	17.45	19.68 (9)	0.02
5,000 Hz.	18.89	22.43 (6)	0.001
Total ms Vel. (20 band)	18.22	22.43 (6)	0.001

The same pattern in Figure 5.8 is shown by other data for the plate. Based on the reasons above, eliminating the contributions from the vicinity of 3-σ region yields hypothesis test result summary for the plate in Table 5.4. Note that the structure plate

failed to pass the hypothesis test. The reason for the failure is that the Lyapunov condition terms for structures are larger than those for spaces.

5.6 Conclusions

Distributions of SEA responses are proven to be Gaussian regardless of distributions of design parameters in this paper. A Monte Carlo test on a three element SEA model was conducted and 2,000 SEA models are generated for each of 20 frequency bands. A statistical hypothesis test was conducted based on the statistical population of the SEA responses. Test results show that SEA responses and total acoustic pressure and structural velocity from SEA obey approximately Gaussian distributions. The results also show that the Gaussian distributions are better approximated to distributions of sound pressures for acoustic spaces than those of the structural velocity for the plate. The reasons are that plate element has a constant modal density (A1, Appendix A) and SEA method works better for high modal density. The Gaussian distributions of SEA responses can be applied to evaluate the confidence levels of the existing acoustic designs and develop specifications for new designs. With these features and applications, the Gaussian distributions for SEA responses provide a powerful design tool for quality acoustic designs for aerospace, ship and automotive vehicles.

Chapter 6 Summary and Conclusions

6.1 Dissertation Summary

This dissertation develops a parameter identification algorithm for internal loss factors. There are no analytical expressions available for damping and they must be determined experimentally. Internal loss factors in each frequency band can be uniquely identified by solving inverse SEA equations given measure acoustic sound pressure and structural velocities in an SEA model. The least square method is then used to determine frequency-independent acoustic reverberation time and structural damping by minimizing the ms errors between identified and computed internal loss factor in each frequency band.

This dissertation presents a sound pressure sensitivity methodology for SEA. From the design point of view, SEA needs the power of not only computing the variability of sound pressure level of an SEA model to variability of physical parameters but also determining which design parameters cause the maximum sound pressure level variation so that those design parameters can be selected which reduce the overall sound pressure level with the least effort. The methodology discussed here allows quantitative prediction of sound pressure sensitivity to variations in SEA design specification parameters. and is able to determine the maximum sensitivity of the sound pressure levels to the design parameters.

This dissertation develops a variance analysis method for SEA to extend the design application of the SEA method through prediction of the variances of RMS responses of vibro-acoustic structures and interior spaces from variances in SEA model physical

parameters. This analytical ability would allow variance analysis of sound and vibration response to the variances of design specifications.

This dissertation shows that probability distributions of SEA acoustic pressure and structural velocity responses are Gaussian. The Gaussian distributions characterize the random features of the sound pressure and velocity and provides a means for predictions of response variances and confidence levels.

6.2 Conclusions

The SEA methodology has been extended in this dissertation to include optimal internal loss factor identification, sound pressure sensitivity analysis, SEA response variance analysis and statistical distribution analysis. These new developments and features increase the power of the SEA method as a tool for vibro-acoustic design and modeling at audio frequencies.

APPENDICES

APPENDIX A SEA EQUATIONS

(1) Modal Density Equations (Lyon, R.H., 1975):

Plate Structure:

$$n_2 = \frac{\sqrt{3}A}{hc_l} \tag{A1}$$

where A is the area of the panel (m^2)

h is the thickness of the panel (m)

c_l is longitudinal wave speed in the panel (m/s)

Acoustic Space:

$$n_1 = n_3 = \frac{4\pi f^2 V}{c^3} + \frac{\pi f A_s}{2c^2} + \frac{L_e}{8c} \tag{A2}$$

where f is the analysis band center frequency (Hz.),

V is volume of the space (m^3)

A_s is the surface area of the space (m^2)

L_e is the edge length of the space (m)

c is the speed of sound in air (m/s)

(2) Coupling Loss Factor Equations (Lyon, R.H., 1975):

From Plate to Acoustic Space:

$$\eta_{21} = \eta_{23} = \frac{\rho c A}{2\pi f M_p} \begin{cases} \frac{2\lambda_c P}{\pi^2 A} \sin^{-1}\left(\frac{f}{f_c}\right)^{1/2} \beta, & f < f_c \\ \left(1 - \frac{f_c}{f}\right)^{-1/2}, & f > f_c \end{cases} \tag{A3}$$

where ρ is fluid density (kg/m^3),

c is the speed of sound in the fluid (m/s),

A is the area of the panel (m^2),

P is the perimeter of the panel (m),

M_p is the mass of the panel (kg)

$f_c = \frac{12.5}{h}$ is the critical frequency (Hz.)

$\lambda_c = \frac{c}{f_c}$ is the wavelength of sound at the critical frequency (m)

$$\beta = \begin{cases} 1 & \text{for simple edge supports} \\ 2 & \text{for clamped edge supports} \\ \sqrt{2} & \text{for typical mounting conditions} \end{cases}$$

$$\eta_i = \begin{cases} 2\zeta & \text{for structures} \\ \frac{2.2}{T_R f_k} & \text{for acoustic space} \end{cases} \quad \text{(A4)}$$

where ζ is damping ratio of flat plate

T_R is reverberation time in acoustic space

For the flanking path between Engine Compartment and Over Car Volume, a constant coupling loss factor is assumed.

$$\eta_{26} = 0.0005 \quad \text{(A5)}$$

Table A1 Geometric and Material Properties Used in Example 1

Longitudinal Wave speed in Plate (m/s)	5181.0
Speed of Sound in Air (m/s)	344
Plate Thickness (m)	0.0007
Length of the Cube (m)	0.5
Air Density (kg/m^3)	1.244
Aluminum Density (kg/m^3)	2700
Speed of Sound in Aluminum (m/s)	6400
Reverberation Time in Space 1 (second)	1.5
Reverberation Time in Space 2 (second)	1.2
Flanking Coupling Loss Factor	0.0001
Damping Ratio in Plate	0.001

APPENDIX B GEO METRO MODEL DATA

B.1. GEO METRO Design Parameters

There are eight (8) elements in the EGO SEA Model. Front of Dash (plate) is numbered as 1, Engine Compartment (acoustic volume) is numbered as 2, Hood (plate) is numbered as 3, Under Car Volume (acoustic volume) is numbered as 4, Floor Panel (plate) is numbered as 5, Over Car Volume (acoustic volume) is numbered as 6, Body Panel (plate) is numbered as 7 and Interior (acoustic volume) is numbered as 8.

Table B1 List of Design Parameters for The GEO SEA Model Body Structures

	element number	thickness (m)	surface area (m^2)	mass (kg)	edge length (m)	longitudinal wave speed (m/s)	length (m)	width (m)	Young's modulus (GPa)
Front of Dash	1	0.0077	0.6368	10	3.1496	5181.7	1.0414	0.5334	190
Hood	3	0.0030	1.2876	40	4.4958	5181.7	1.3208	1.0541	190
Floor Panel	5	0.0038	4.111	180	8.4836	5181.7	2.7432	1.4986	190
Body Panel	7	0.0038	9.7711	340	53.996	5181.7	3.12	3.12	190

Note that the thicknesses for structural elements in the GEO SEA model are the effective thickness which are obtained by multiplying the nominal thicknesses with an effective factor. The effective factor is introduced to take care of local stiffener, add-on structures and curvatures on plates. The effective factor here is taken as 2 to 5.

Table B2 List of Design Parameters for The GEO SEA Model Acoustic Spaces

	element number	volume (m^3)	surface area (m^2)	edge length (m)	medium density (kg/m^3)	speed of sound (m/s)
Engine compartment	2	0.6368	10	3.1496	1.244	344
under car volume	4	1.2876	40	4.4958	1.244	344
over car volume	6	4.111	180	8.4836	1.244	344
interior	8	9.7711	340	53.996	1.244	344

B.2. GEO SEA Model Connectors

There are 16 connectors in the GEO SEA Model. There is a flanking path between engine compartment and over car volume. The plate to acoustic space connectors are listed in Table B3, the plate to plate connectors are list in Table B4 and the space to space connector is listed in Table B5.

Table B3 List of Connectors between panels and spaces for The GEO SEA Model

element numbers between a connector	Fixation β
1,2	$\sqrt{2}$
1,8	$\sqrt{2}$
2,3	$\sqrt{2}$
2,7	$\sqrt{2}$
3,6	$\sqrt{2}$
4,5	$\sqrt{2}$
5,8	$\sqrt{2}$
6,7	$\sqrt{2}$
7,8	$\sqrt{2}$

Table B4 List of Connectors between panels for The GEO SEA Model

element number between a connector	connection angle (degree)	connection length (m)
1,3	70	1.3462
1,5	90	1.0414
1,7	90	2.0
3,7	90	2.0828
5,7	90	6.985

Table B5 List of Space to Space Connector for The GEO SEA Model

element number between a connector	coupling area (m^2)	sectional area (m^2)
2,4	90	6.985

B.3. GEO METRO Test Results

The body was excited by 0.9 V amplitude random noise signal from HP 35660A Dynamic Signal Analyzer respectively. The accelerations for structural elements are in dB referring to 1 g and SPL for acoustic spaces has standard pressure reference $P_{ref} = 20\mu P_a$.

Table B6 List of Measured Acceleration and SPL of State 1 for GEO SEA Model

element number	1	2	3	4	5	6	7	8
third octave band center frequency (Hz.)	dB	dB	dB	dB	dB	dB	dB	dB
500	-29.35	64.99	-53.94	57.89	-56.75	58.50	-61.02	66.66
630	-28.20	63.93	-52.54	60.07	-53.29	59.27	-58.69	64.46
800	-23.18	68.51	-45.92	62.61	-48.00	63.38	-56.96	67.52
1000	-16.95	75.52	-42.62	70.49	-43.48	71.49	-51.54	69.47
1250	-15.58	77.69	-39.55	70.53	-40.45	71.85	-52.85	70.60
1600	-8.89	82.31	-34.34	75.22	-31.54	75.76	-50.68	72.80
2000	-20.14	71.29	-48.66	64.25	-45.58	63.74	-61.72	60.04
2500	-30.72	68.41	-54.41	63.19	-54.04	58.34	-63.46	56.33
3150	-32.65	82.91	-44.72	73.49	-49.40	70.55	-59.59	60.79
4000	-24.05	76.20	-50.78	69.01	-53.47	65.13	-61.81	58.53
5000	-26.55	80.82	-49.32	75.02	-54.51	69.96	-60.37	59.36

Table B7 List of Measured Acceleration and SPL of Operating State 2 for The GEO SEA Model

element	Dash Panel	Interior
third octave band center frequency (Hz.)	dB (re 1 g)	dB
500	-28.13	68.13
630	-25.25	66.49
800	-28.47	63.57
1000	-22.92	64.83
1250	-19.53	67.46
1600	-11.61	70.26
2000	-26.40	59.88
2500	-34.29	52.96
3150	-34.79	51.28
4000	-32.18	51.65
5000	-33.23	52.82

B.4. Model Predictions and Comparison

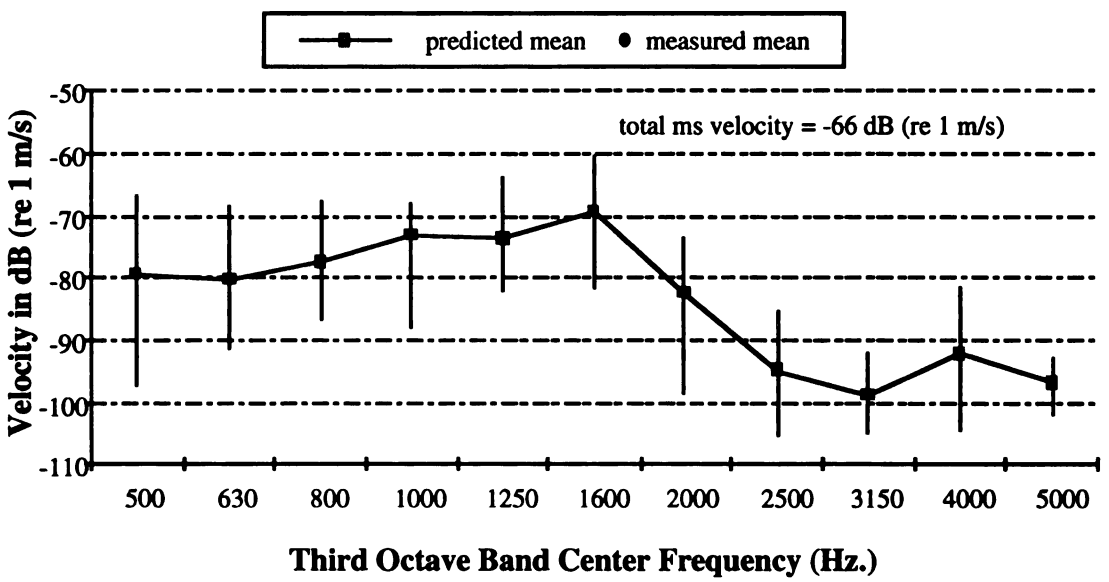

Figure B1 GEO Front of Dash Velocity Prediction and Measurement

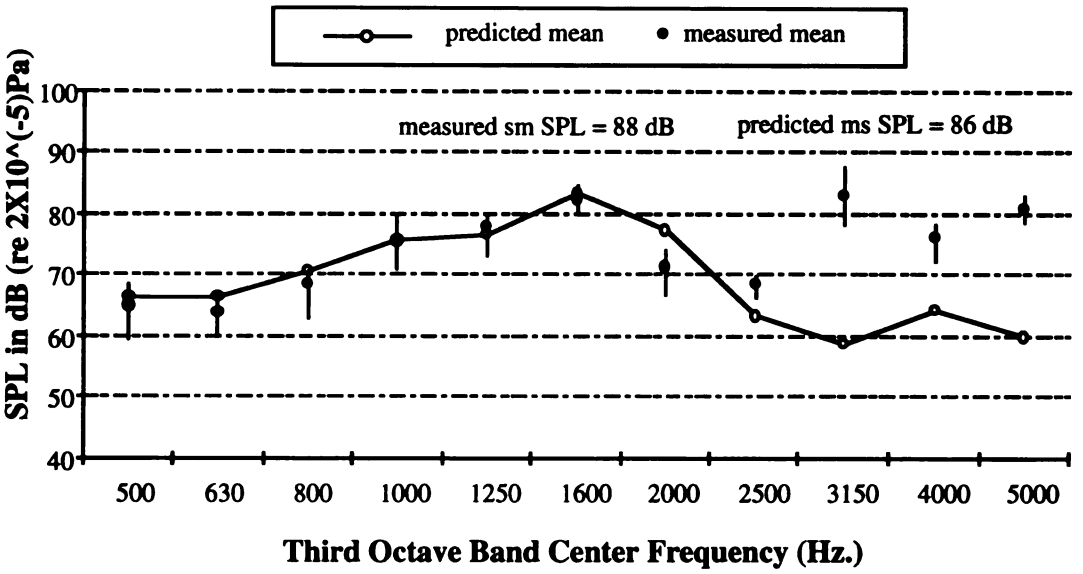

Figure B2 GEO Engine Compartment SPL Prediction and Measurement

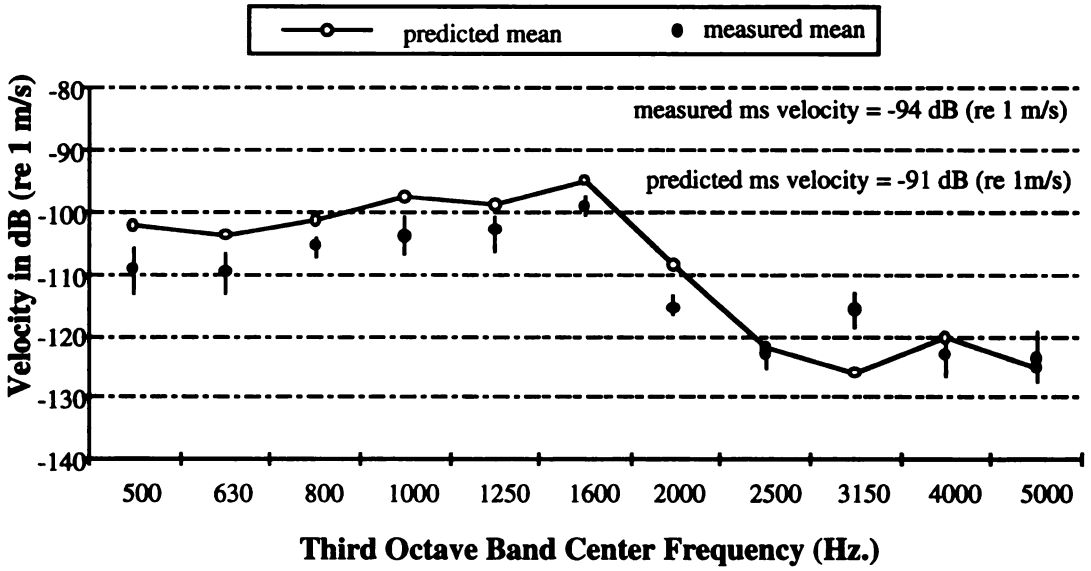

Figure B3 GEO Hood Velocity Prediction and Measurement

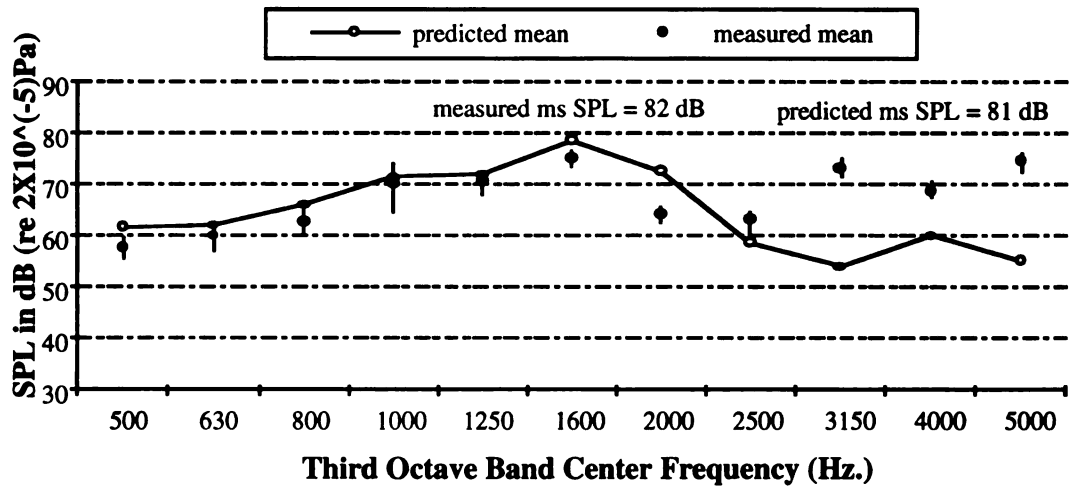

Figure B4 GEO Under Car Volume SPL Prediction and Measurement

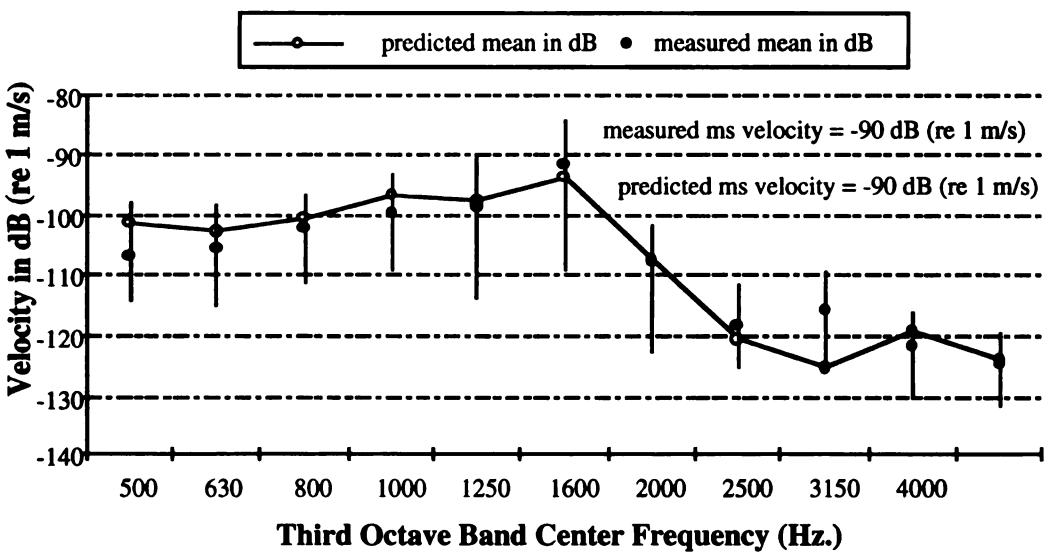

Figure B5 GEO Floor Panel Velocity Prediction and Measurement

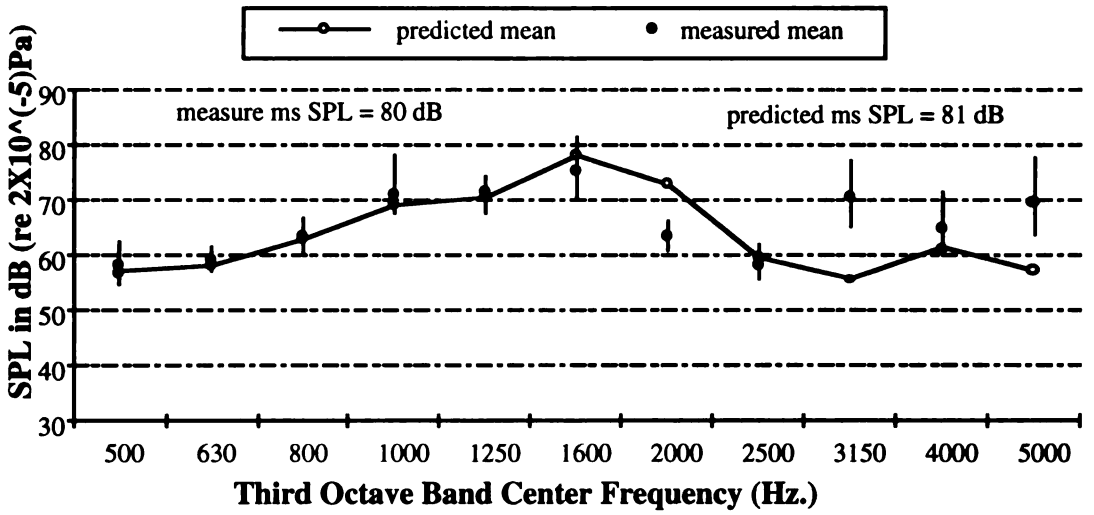

Figure B6 GEO Over Car Volume SPL Prediction and Measurement

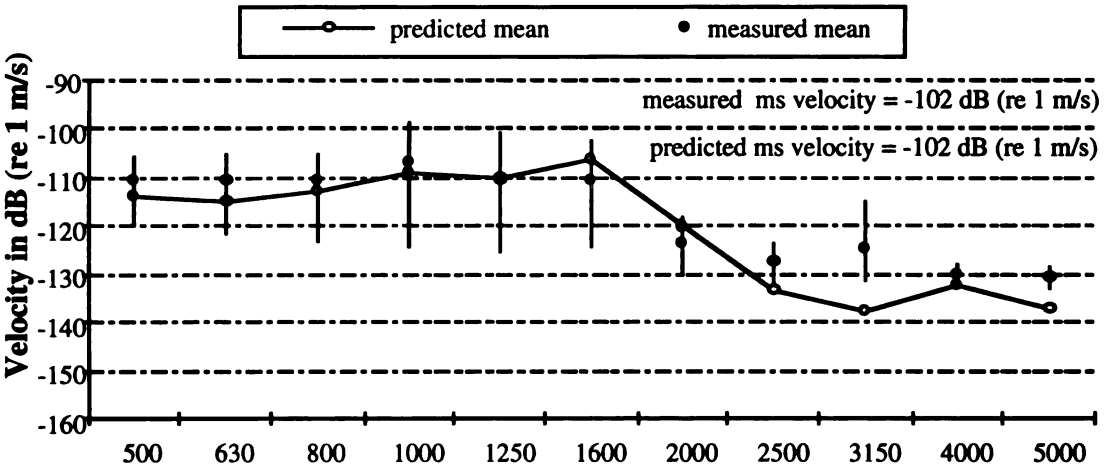

Figure B7 GEO Body Panel Velocity Prediction and Measurement

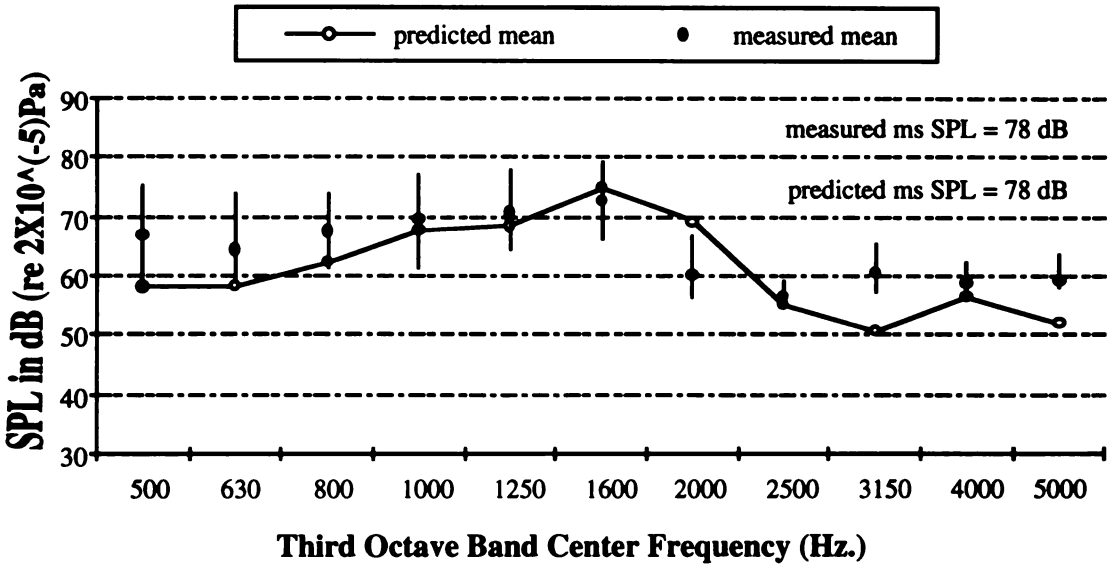

Figure B8 GEO Interior SPL Prediction and Measurement

BIBLIOGRAPHY

BIBLIOGRAPHY

Bies, D.A. and Hamid, S., 1980, In Situ Determination of Loss and Coupling Loss Factors by The Power Injection Method, *Journal of Sound and Vibration*, Vol. 70, No. 2, pp.187-204,

Clarkson, B.L. and Pope, R.J., 1981 Experimental Determination of Modal Densities and Loss Factors of Flat Plates and Cylinders, *Journal of Sound and Vibration*, Vol.. 77, No. 4, pp. 535-549

Clifford, A.A., 1973, Multivariate Error Analysis, A handbook of Error Propagation and Calculation in Many-Parameter Systems, Halsted Press.

Cramér, H., 1963, *Mathematical Methods of Statistics* , Princeton University Press, Princeton

DeJong, R. G., 1985, "A Study of Vehicle Interior Noise Using Statistical Energy Analysis, " SAE Paper No. 850960

Frank, P. M., 1978, *Introduction to System Sensitivity Theory* , Academic Press, New York

Ghering, W.L. and Raj, D., 1987 "Comparison of Statistical Energy Analysis Predictions with Experimental Results for Cylinder-Plate-Beam Structures," *Statistical Energy Analysis*, Edited by Hsu, K.H. and Nefske, D.J. and Akay, A., NCA-Vol.3, ASME, N.Y., N.Y.

Hodges, C.H., Nash, P., and Woodhouse, J., 1987, " Measurement of Coupling Loss Factors by Matrix Fitting: An Investigation of Numerical Procedures," Applied Acoustics, Vol. 22, pp. 47-69

Huang, X.L. and Radcliffe, C.J., 1993, "Sensitivity of The Statistical Energy Analysis for Automotive Vehicles", Paper No. WAM93-18, The 4^{th} Symposium on Advanced Automotive Technologies of the 1993 ASME Winter Annual Meeting, New Orleans, Louisiana, USA

Jacobs, R.H., Yoerkie, C.A., Gintoli, P.J., and Manning, J.E., 1989, "Statistical Energy Analysis Modeling of the Sikorsky ACAP Helicopter," *Analysis Techniques in Acoustics* Edited by Hsu, K.H., and Keltie, R.F., NCA-Vol.9, ASME, N.Y., N.Y.

Jenson, J.O. ,1979, "Prediction of Noise in Ships by the Application of "Statistical Energy Analysis," *J. Acoustic. Soc. Am.*, Vol. 66(S1), S4(A).

Kompella, M.S. and Bernhard, R.J., 1993, "Measurement of the Statistical Variation of Structural-Acoustic Characteristics of Automotive Vehicles," *Proceedings of the 1993 Noise and Vibration Conference* , SAE P-264, pp.65-82

Lu, L.K.H. and et. al., 1983, "Comparison of Statistical Energy Analysis and Finite Element Analysis Vibration Prediction with Experimental Results," *The Shock and Vibration Bulletin*, May, No. 53, Part 4, pp.145-154.

Lu, L. K. H., 1987, "Optimum Damping selection by Statistical Energy Analysis," *Statistical Energy Analysis*, Edited by Hsu, K. H., Nefske, D.J. and Aka, A., NCA-Vol. 3, ASME, N.Y., N.Y.

Lyon, R.H. and Maidanik, G., 1962, "Power Flow between Linearly coupled Oscillators," *J. Acoustic. Soc. Am.*, May, Vol. 34, No. 5, pp. 623-639.

Lyon, R.H., 1975, Statistical Energy Analysis of Dynamical Systems: Theory and Applications, MIT Press, Cambridge, Mass.

Lyon, R.H., 1987, "The SEA Population Model - Do We Need a New One?," *Statistical Energy Analysis*, Edited by Hsu, K.H., Nefske, D.J. and Aka, A., NCA-Vol.6, ASME, N.Y., N.Y.

Norton, M.P. and Greenhalgh, R., 1986 "On the Estimation of Loss Factors in Lightly Damped Pipeline Systems: Some Measurements Techniques and Their Limitations," *Journal of Sound and Vibration*, Vol. 105, No. 3, pp. 397-423

Oh, H.L., 1987, "Variation Tolerant Design," *Quality: Design, Planning, and Control,* Edited by DeVor, R.E., and Kapoor, S.G, PED-Vol. 27, ASME, N.Y., N.Y.

Powell, R.E. and Quartararo, L.R., 1987, "Statistical Energy Analysis of Transient Vibration ," Statistical Energy Analysis, K. H. Hsu et al, ed., NCA-Vol. 3, ASME, N.Y., N.Y.

Radcliffe, C. J. and Huang, X. L., 1993, "Putting Statistics into the Statistical Energy Analysis of Automotive Vehicles," Vibration Isolation, Acoustics, and Damping in Mechanical Systems, DE-Vol. 62, C.D. Johnson, et al, ed., ASME book G00823, pp. 51-60

Radcliffe, C. J. and Huang, X. L., 1993, "Identification of Internal Loss Factors During Statistical Energy Analysis of Automotive Vehicles," Proceedings of the 1993 Noise and Vibration Conference, SAE P-264, pp. 311-318.

Remington, P.J. and Manning, J.E., 1975, "Comparison of Statistical Energy Analysis Power Flow Predictions with an 'Exact' Calculation," *J. Acoustic. Soc. Am.*, Feb., Vol. 57, No. 2, pp. 374-379.

Smith, P.W. Jr., 1962, "Response and Radiation of Structural Modes Excited by Sound," *J. Acoustic. Soc. Am.*, May, Vol. 34, No. 5, pp. 640-647.

Yoerkie, C.A., Moor, J.A., and Manning, J.E., 1983, " Development of Rotorcraft Interior Noise Control Concepts - Phase I: Definition Study," NASA Contractor Report 166101

Lyon, R.H., 1967, "Statistical Analysis of Power Injection and Response in Structures and Rooms," *J. Acoust. Soc. Am.* , **45**, No. 3, pp. 545-565

Volk, W., 1969, *Applied Statistics for Engineers*, 2nd ed., McGraw-Hill Book Company, New York

Vail, C.F., 1972 "Dynamics Modeling of Automobile Structures from Test Data," *System Identification of Vibrating Structures*, Edited by Pilkey, W.D. and Cohen, R., ASME, N.Y., N.Y.